Cancer Detection Using Printed Antenna Placed on Human Breast Model

Nagia Rafalla Ali

Submitted to the
Institute of Graduate Studies and Research
in partial fulfillment of the requirements for the degree of

Doctor of Philosophy
in
Electrical and Electronic Engineering

Eastern Mediterranean University
September 2020
Gazimağusa, North Cyprus

Approval of the Institute of Graduate Studies and Research

Prof. Dr. Ali Hakan Ulusoy
Director

I certify that this thesis satisfies all the requirements as a thesis for the degree of Doctor of Philosophy in Electrical and Electronic Engineering.

Assoc. Prof. Dr. Rasime Uyguroğlu
Chair, Department of Electrical and Electronic Engineering

We certify that we have read this thesis and that in our opinion it is fully adequate in scope and quality as a thesis for the degree of Doctor of Philosophy in Electrical and Electronic Engineering.

Prof. Dr. Abdelmegid Allam
Co-Supervisor

Assoc. Prof. Dr. Rasime Uyguroğlu
Supervisor

Examining Committee

1. Prof. Dr. Serkan Aksoy
2. Prof. Dr. Abdelmegid Allam
3. Prof. Dr. Hasan Demirel
4. Prof. Dr. Osman Kükrer
5. Prof. Dr. Mehmet Siraç Özerdem
6. Prof. Dr. Şener Uysal
7. Assoc. Prof. Dr. Rasime Uyguroğlu

ABSTRACT

In this study electromagnetic properties of female human breast were used for cancer tissue detection. Deviation of the malignant cells' properties from those of healthy cells' directly affect the performance of an antenna placed on the breast. Return loss, gain and directivity of an antenna designed on an FR4 substrate were used as parameters for studying the effects of the normal and cancerous tissues. Planar and hemispherical shaped, multilayer breast models, composed of skin, fat and part of the connected lymph nodes were modeled and designed. The antenna was designed, fabricated, and return loss measurements were taken by a network analyzer (Rohde & Schwarz ZWB20). Separate measurements were taken in free space and when placed on a healthy human breast.

Simulations of normal breast models carried out by CST Microwave Studio were in a good agreement with the measured results.

Tumors in breast and lymph nodes with different sizes and numbers defined according to American Joint Committee on Cancer (AJCC) were used to model the first and second stages of cancer.

The presented work is shown to be a promising method for breast cancer studies, thereby reducing the need for invasive surgical operations.

Keywords: Breast cancer, Microstrip antenna, Biomedical.

ÖZ

Bu çalışmada, kadın memesinin elektromanyetik özellikleri ile elektromagnetik alanlar kanserli doku tespiti için kullanılmıştır. Kötü huylu hücrelerle sağlıklı hücreler arasındaki elektriksel farklılıklar, meme üzerine yerleştirilen antenin performansını farklı şekilde etkilemektedir. Bu amaçla FR4 materiyal kullanılarak bir anten tasarlanmıştır. Meme üzerine yerleştirilen antenin, geri dönüş kaybı, kazanç ve yönlülük gibi parametreleri incelenerek normal ve kanserli dokular arasındaki farklılıklar ortaya konmuştur.

Deri, yağ dokusu ve lenf bezlerinin bir kısmını kapsayan düzlemsel ve yarım küre şeklinde iki farklı meme modeli kullanılarak benzetim çalışmaları yapılmıştır. Ayrıca, tasarlanan anten üretilmiş ve bir ağ çözümleyicisi (Rohde & Schwarz ZWB20) ile normal kadın memesi üzerinde ve hava ortamında geri dönüş kaybı ölçülmüştür, benzetim sonuçları ile karşılaştırma yapılmıştır.

American Joint Committee on Cancer (AJCC) tanımına göre, meme kanserinin birinci ve ikinci evresi ile ilgili farklı boyut ve sayıdaki meme ve lenf bezi tümörleri modellenerek benzetim sonuçları elde edildi.

Normal kadın memesi üzerine yerleştirilen anten ve CST Mikrodalga Simülatörü kullanarak, tasarlanan aynı özellikteki normal kadın memesi modelinden elde edilen geri dönüş kayıbı sonuçları iyi bir uyum içerisindedir. Ancak, kanserli doku içeren kadın memesi üzerinde ölçüm gerçekleştirilememiş, sadece benzetim sonuçlarına dayalı bir çalışma yapılabilmiştir.

Sunulan çalışma geliştirilmesi durumunda, meme kanseri tespiti için gerekli invazif cerrahi işlemlere olan ihtiyacı azaltıcı yararlar sağlayacaktır.

Anahtar Kelimeler: Meme kanseri, Mikroşerit anten, Biyomedikal.

ACKNOWLEDGEMENT

Foremost, I would like to express my sincere gratitude to my supervisors Prof. Dr. Rasime Uyguroğlu and Prof. Dr. Abdelmegid Allam for their continuous support, patience, motivation and immense knowledge. Nothing of this could be achieved without their help and support.

I would like to thank my husband, my children, my sister, and my friends who always supported me.

TABLE OF CONTENTS

LIST OF TABLES

LIST OF FIGURES

LIST OF SYMBOLS

B	Magnetic field flux density
c_0	The speed light in free space
E	Electric field intensity vector
f_r	Resonant frequencies
G	Conductance
H	Magnetic field intensity vector
L_{eff}	Effective length
p_{rad}	Radiated power
R_r	Radiation impedance
Y	Complex propagation constant
δ_{eff}	Effective loss tangent
ε	Permittivity
ε_r	Relative permittivity
η	Wave impedance
λ	Wavelength
μ	Relative permeability
σ	Electric conductivity
Ω	Ohm

LIST OF ABBREVIATIONS

ANSI	American National Standards Institute
BAN	Body Area Network
BW	Bandwidth
CST	Computer Simulation Technology
EIRP	Equivalent Isotopically Radiated Power
EM	Electromagnetic
EMC	Electromagnetic Compatibility
EMI	Electromagnetic Interference
ERP	Equivalent Radiated Power
ETSI	European Telecommunications Standards Institution
FCC	Federal Communication commission
FDTD	Finite Difference Time Domain
FM	Frequency Modulation
FR-4	Flame Retardant 4
HBC	Human Body Communication
HF	High Frequency
IBC	Intra Body Communication
IEEE	Institute of Electrical and Electronic Engineers
IMD	Implantable Medical Devises
ISM	Industrial Scientific and Medical
LF	Low Frequency
MICS	Medical Implants Communication System
PIFA	Planar Inverted – F Antenna

RF	Radio Frequency
SAR	Specific Absorption Rate
SMA	Sub Miniature version A
UWB	Ultra Wide Band
WBAN	Wireless Body Area Network

Chapter 1

INTRODUCTION

In recent years, biomedical engineering applications and the devices to be used for these applications attract the attention of the researchers in the field. Using devises in (implant) or on a human body has an important role for diagnosis and treatment processes of serious diseases since it helps reducing the invasive surgical operations. In the same time, these devices are considered as a main brain stone in a communication link [1] between the implantable devises in the body and the outside world (doctor, hospital, medical center or data storage in a network).

When such a device is to be used, the electrical properties of it are taken into consideration in order to achieve better matching between the human body and the device. The electrical properties of the implant are also play an important role in the power loss and also with its physical dimension as well.

One of the severe and fatal disease is known to be the breast cancer, being commonly diagnosed worldwide especially for women. Based on the National Cancer Institute's old estimation report 2013, 40,030 breast cancer deaths [2] happened up to this year. A huge number of women belong to the age group of 25 – 40 years, suffered from breast cancer leading to the need for the initial detection. It is also shown in literature that this of number decreases, if the process of early detection is being used. Medically, a mammogram is an old and up till now is the technique used for

breast cancer detection. Unfortunately, the method is not very efficient especially for dense breasts; also the patient should be exposed to x-rays. So, researchers should propose some other scenarios for the early breast cancer detection. In this thesis the proposed work is based on the contrast in the dielectric properties between normal and malignant tissues of human body. This technique is based on the electric and magnetic properties of the human tissues and how one can use it for early detection of cancer.

1.1 Thesis Objective

The objective of this thesis is to make a scenario for early detection of cancer in breast depending on the marginal differences between the electrical properties for both the normal and malignant tissues of the human breast.

A low profile, cheap and small size printed patch antenna is used on breast for the sake of cancer detection. The antenna comprises different bricks of copper annealed implemented and fabricated on FR4 substrate with relative dielectric constant 4.3, thickness 1.6mm and loss tangent 0.025 with overall antenna dimensions 5×4 cm^2. It is excited using microstrip line of 50 Ω for good matching with the source. Two human breast models are illustrated for cancer detection, based on the definition of [2], in stage I and stage II.

1.2 Thesis Contribution

In this study, biomedical stages of cancer, depending upon the tumor size, number and location are used for breast cancer detection in early stages to be used for further investigations by specialists.

The constitutive parameters (σ, μ, Ɛ) of the human breast at the ISM frequency band are used for designing the breast models.

As a thesis contribution, the following achievements can be listed:

a) Designing, fabricating and taking measurements with an antenna designed for this purpose, which is in the form of a patch, comprising of different strips like patch antenna.
b) Implementing this algorithm on two different human breast models:
    i) Planar breast model,
    ii) Spherical breast model,
c) Using antenna parameters like return loss, gain and directivity to differentiate the normal breast from the tumorous breast.

1.3 Thesis Organization

The thesis consists of six chapters including the Introduction. Chapter 1 gives a motivation and a glossary of the work done on this thesis. Chapter 2 is devoted to the outlines of an antenna placed on/in a human body and its frequency bands. In addition, the challenges of implanting antennas are addressed. Some phantoms of different human organs are also presented with some typical antennas that have been used in implantation. The theory and analysis of microstrip antenna is summarized in Chapter 3. The design details of the printed antenna adopted in this work are illustrated through Chapter 4. The antenna is placed on a normal model of the human breast and studied for cancer stages 1A and 1B. The scenario of detecting cancer for these stages is presented. Concerning the novel breast model, Chapter 5 presents an application of the adopted implanted antenna on the model which is used for the

breast cancer detection of stage 2. The work is concluded in Chapter 6 with some highlights for future work.

Chapter 2

OUTLINES ON IMPLANTED ANTENNAS

2.1 Introduction

The use of implantable devices for biomedical applications has grown significantly [5-7]. These devices can be implanted for the sake of detection of diseases by sensing some signs like temperature, blood flow, glucose level, etc. within a human body and hence, can send them to another device used by specialists or doctors for diagnosis and treatment. The outward device is placed either near to the body of the person (close to the field area of the antenna) as shown in Figure 1, or around some meters away (faraway of the area of the antenna) as in Figure 2.

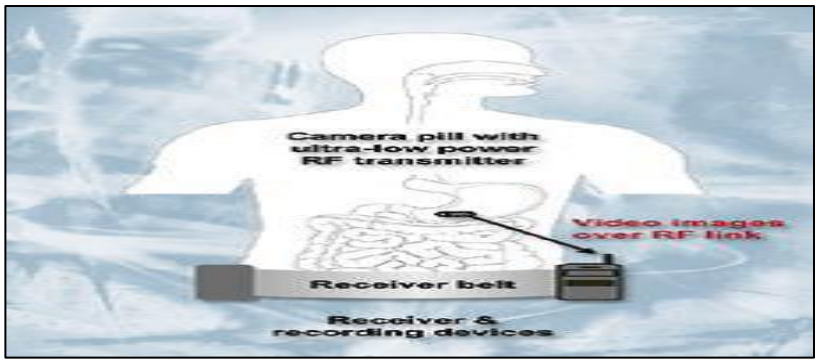

Figure 1: Attachable receiver and recording device of wireless Pill endoscopy [8]

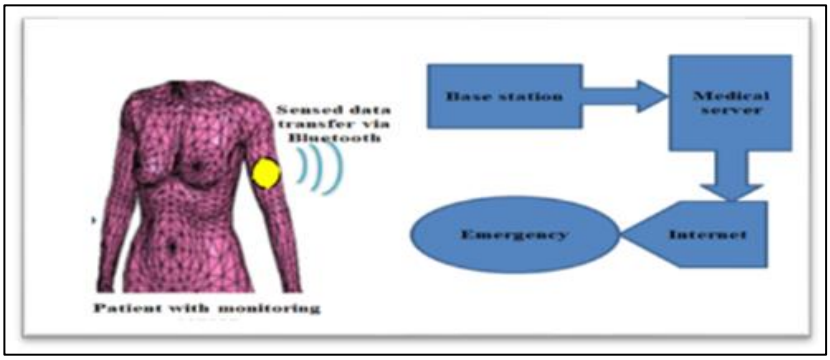

Figure 2: Health examination structure

The data obtained from the outside device can be monitored by some smart units and doctors dedicated to the patient, as appeared in Figure 1. This allows some infections, like growth or polygenic disease, to be analyzed in their initial stages, whereas basic therapeutic conditions, like heart attacks or strokes, will be anticipated and hindered [7]. This can be additionally extraordinarily appropriate, for frameworks of human services, to observe a couple of bio-physical factors, like the glucose level.

In reality, numerous gadgets, for example, pacemakers, implantable glucose antennas have exhibited the significance of these devices in curing and wellbeing check in [7]. The implantable device is made out of ~~a~~ few segments, for example, sensors, a battery, and antennas.

An example of an implantable gadget is shown in Figure 3. In the center part, the reception apparatus is the largest part and creates the connection between the bodies of the individual to an outer collector. It can be observed that, the antenna presents an essential part in the general weight and size diminishment of the implantable device.

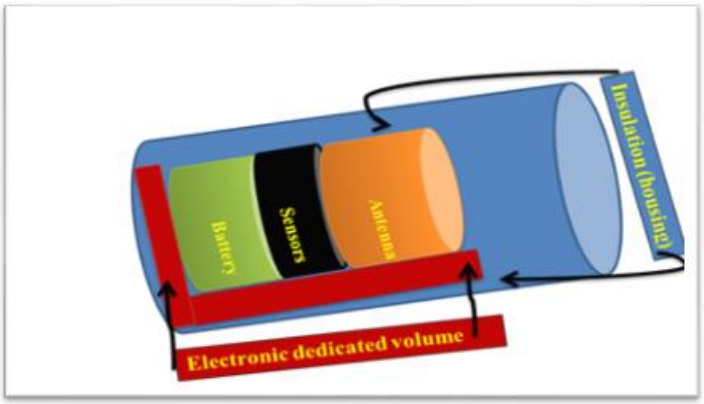

Figure 3: Implantable gadget

Implanted antennas are antennas which are either implanted inside or outside a human body used for diagnosis, analysis and treatment. Basically, in treatment the implanted antennas can be used to increase the temperature of the malignant tissues. So the antenna shape, structure and parameters are different if it is inside or outside the body and where it is implanted [9-11].

It should be pointed out that the implanted antenna is considered as a pivot element in a design of a communication link between the implanted device and the receiving item either, hospital, doctor, mobile, etc. On the other hand, nowadays it is a crucial point of research in biomedical engineering exploration because saving the body from surgery is of high importance for human life. That is to say, in order to reduce the need of surgical operations, implanted devices are used as a part of diagnosis and treatment process [1].

One can say that the focus of study in this region is how to produce hyperthermia for medical porposes and how to monitor the physiological parameters in the human bod y are the most prevalent in medical application research [1].

2.2 Frequency Band of Implanted Antennas

There are two standards used as a frequency band of implanted antennas inside human body which are MICS band and ISM band.

2.2.1 MICS Standard

The Medical Implant Communication Service (MICS) has standardized by the European Telecommunications Standards Institute (ETSI). Two lists of applications are documented. The first one is for telecommunication between an implanted device and a base station. The second one is for telecommunication between medical implants within the same body. The assigned frequency band is 402 MHz to 405 MHz with bandwidth 300 kHz. The MICS band was considered well for the service, due to the signal propagation characteristics in the human body [12]. Low-power regime is recommended to be used for MICS band, so, an ultra-high performance transceiver is required.

2.2.2 ISM Standard

The Industrial, Scientific and Medical (ISM) band (2.4 GHz to 2.4835 GHz) is a band to be used for medical implant communication. It is the same band that is used by Wi-Fi, Bluetooth, cordless telephones and household microwave ovens. The maximum effective isotropic radiated power, EIRP is -10 Dbw (100 Mw). The system should be spread spectrum, either Frequency Hoping Spread Spectrum (FHSS) or Direct Sequence Spread Spectrum (DSSS). For FHSS, we should use at least 15 separate non-overlapping channels while for DSSS, the maximum power density is -20Dbw/MHz EIRP. The main drawback of this band is that it is shared with all the other users of the same band which force the need of on inter-operability and security. We should point out that the penetration into the human body of this band is less than the penetration at 400 MHz [12].

2.3 Challenges of Implanted Antenna

Placing an antenna inside a human body will come up with many challenges, simply the immune system of the human body fights with any foreign object. The shape, size, and type of an antenna is to be designed according to the body organ that an implant is required. For example an antenna placed inside the eye will not have the same requirement for another one placed in the arm or just under the skin. In addition, the surrounding organ will change the antenna parameters. In this section some forthcoming challenges for implanted antennas shall be covered, and solutions will be proposed for overcoming them.

2.3.1 Scalable Design

Antennas can be implanted in different body parts, performing different tasks. Therefore, it is convenient to determine the antenna design parameters, and its shape according to the body organ and the functionality. For example, helical antenna would be used for urinary application, a microstrip antenna would be used in the chest or head, also a waveguide antenna would be placed externally while a dipole or monopole antennas are placed internally. Another important aspect in designing the antenna would be the dimension. An implanted antenna inside the eye must be much smaller than another implanted in the abdomen. Also, some antennas may have the size of a pill for swallowing.

2.3.2 Power and Power Consumption

Power consumption of implanted antenna is very important and should be taken into consideration in the design process. It has been standardized for the MICS band that the maximum effective isotropic radiated power (EIRP) limit is $25\mu W$ [13]. It is clear that low power and less power consumption techniques should be considered, so both topics will be addressed in this subsection.

Regarding the power providing sources: one way is to use the solar energy to provide the needed power. Another possible suggestion is to use the motion of the patient for power generation. It can be done by wearing a special piezoelectric material such that the stress made is converted into electric energy, yet these ideas lack the way of transferring the energy to the implanted antenna. One way of the transfer may be wirelessly. Since energy travels in waves so it may be suggested to use inductance from radio frequencies (RF) or infra-red (IR) signals [14].

Integrating a battery within the implanted antenna is one practical method, although it would provide power for limited time, consequently researches were made to figure out possible ways to enhance the battery life. The power consumption highly depends on the operation of the implant itself. Taking a look on the cardiac pacemaker for example, one would find that the pacemaker only consumes half of the battery's power for the cardiac simulations while the other half is for monitoring, which does not require high power. Lithium iodine battery is a fine choice for implanted devices. It is capable of surviving up to ten years, in addition to the fact that five million lithium iodine batteries have been used in pacemakers for the past four decades [15]. As noticed, for many cases the implanted devices are not required to work the whole time. Using an RF transceiver, it can be switched off, by that consuming less power, and using the ISM band to transmit a signal when needed to operate the device, such strategy would help save power [8]. Inductive coupling is one possible suggestion also. A device like the transformer consists of a primary and secondary coil used to couple the energy. The size of the coils influences the frequency selection and the maximum allowable coupling distance. As it can be seen in Figure 4 the two coils are coupled by their mutual inductance through the tissue

[16]. Mutual induction M = e_m/ (Di / dt), where, e_m is the voltage induced in the coil and I is the current flowing in the coil.

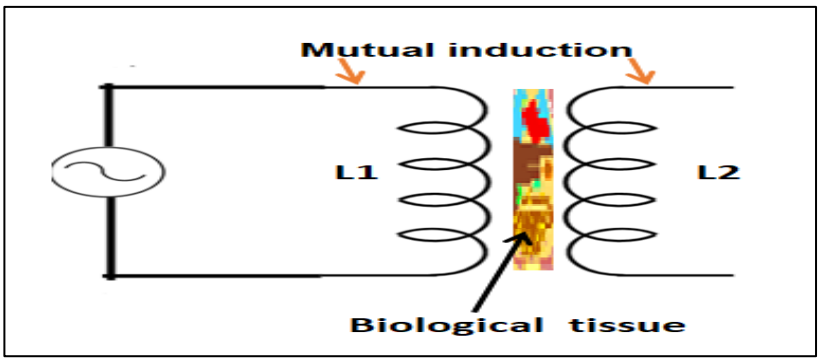

Figure 4: Inductance coupling

Obviously, the power consumption for implanted antennas is a very critical topic, therefore consumption by the implanted antenna should be limited as much as possible. Thus, the less data transferred, the less consumed power. Hence data or image compression could be useful. Another handy technique called “Data Fusion “could be employed in case of more than one implanted antenna, in which data from all implants would be combined and transferred once [14].

2.3.3 Material Restriction

Implanted antenna can be placed inside the body in two ways. Either the implanted antenna will be directly touching the tissues, or it will be packed in a buffer to avoid direct contact [13], as shown in Figure 5.

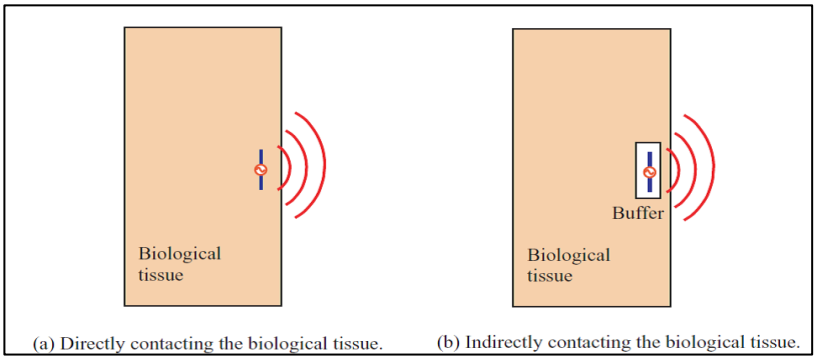

Figure 5: Two ways to place implanted antennas in the body [13]

A serious challenge is having the implanted device formed by using bio-compatible material that will not be rejected by the human body. These materials should be nontoxic and ultra-safe for the surrounding human tissues. For instance, they should have the ability to separate between the implants and the body fluids preventing possible interactions between the biological tissues and the device, without affecting the operation of the device. Also, it should be taken into consideration that platelets from the blood can coagulate on the surface of the implanted device affecting its mission. The potential leakage of substances may harm the surrounding tissues. Another important property for bio-compatible material is their thermal property as any increase in the heat where the implant is placed could affect the tissues.

The importance of packing the implanted antennas by bio-compatible materials like: ceramics, synthetic polymers is clear from the stated problems arise. Silk is another good choice; glass is good for packing and dissipates less power. Aluminum nitride or diamond grown on a silicon substrate would be fine selection as they have good thermal conductivity. Although latter does not have an oxidation layer making it possible to interact with the iron in the human body, so aluminum nitride would be more inert to the body tissues [14].

The privileges of packing the antenna rather than the direct contact with the biological tissues is discussed above. A layer of coat can be applied to the implanted antenna to improve the gain [17].

Polymers

Polymers are considered as bio-compatible materials, because they have some benefits over the other materials, so they are suggested option lately. Polymers are used either in biocompatible materials as packing materials, or in biodegradable materials as in drug delivery ones. Polymers are flexible in fabrication. They offer variable dielectric constants. They provide comfort to the patient when implanted. The permittivity and conductivity of polymers are 80 and 0.7S/m respectively. Packing antenna with biocompatible polymers would reduce its effect on the surrounding tissues. Some polymer types are as follow:

- Thick biocompatible elastomeric is a polymer type used in coating in which the distance between the antenna and the tissue increases, resulting in less harmful effect for surrounding tissues.
- Polyimide materials and Teflon can be used as substrate material, where it exhibits lower loss tangent < 0.00031 at MHz.
- Polydimethyl Siloxane (PDMS) is another polymer type. It was found to be biocompatible, with low permittivity equal to 2.65 and a low loss tangent equal to 0.001 at 100 kHz. Its thickness can reach several hundred micrometers, and can be controlled as well. The drawback of this material is the poor adhesive properties with metals. Surface modification yet can be achieved [18].

2.3.4 Interference

Another challenge that is supposed to arise in time is the interference. As the various types of implanted antennas for medical applications increase, the number of users/patients will also increase. So it is very likely to have more than one patient with an implanted antenna in his/her body which can lead to a possible interference problem between patients. Additional way of interference can come from wireless communication devices such as microwave ovens. The antenna could operate in the MICS band to overcome this type of interference, though its drawbacks were listed earlier. Researchers working to overcome this challenge are still in progress, but no optimum solution is found until now [14].

2.4 Location of Implanted Antennas

There are two ways to put antenna, inside the human body as wire or planar antenna, or outside the body on its surface. Planar or conformal antennas can be designed to put outside the body [1].

Many different numerical techniques can be used for solution and analysis of implanted antennas located inside the human body such as Spherical Dyadic Green's Function (DGF) or Finite Difference Time Domain (FDTD) method. In this study CST, Microwave Simulation Software is used. CST package is based on Finite Integration Technique (FIT).

2.4.1 Finite Integration Technique

FIT is a technique derived by using the combination of Finite Element Method (FEM) and Transmission Line Matrix (TLM) Method. Using more than one numerical technique in one solver, allows it to be used for different applications. This method can easily be used for the solution of complex electromagnetic problems

possessing inhomogeneous materials and irregular structures. A human body is such an electromagnetically complicated structure which consists of various biological tissues including skin, bone, internal organs, etc. FIT is commonly used to study the electromagnetic interactions between implanted antennas and a human body. Also it is used to design the miniaturized antennas to be able to operate in the complex environment of human body [1].

FIT Simulation

To simulate implanted antennas in a human body, an input file for FIT codes needed to be prepared. The first step is to make an anatomical body model which is read by a FIT computer code and the second is to locate implanted antennas inside the body model as shown in Figure 6. By using the tissue information, the proper electrical parameters such as permittivity, conductivity and permeability are defined. Antennas are located and operated inside a human body by applying specific information (the shape, location, input values) of the structures. The electric and magnetic fields are updated by the solver. The human body model at 402 MHz, 2.4GHz and 2.5GHz with its electrical data of biological tissues used are tabulated in Section 2.5.

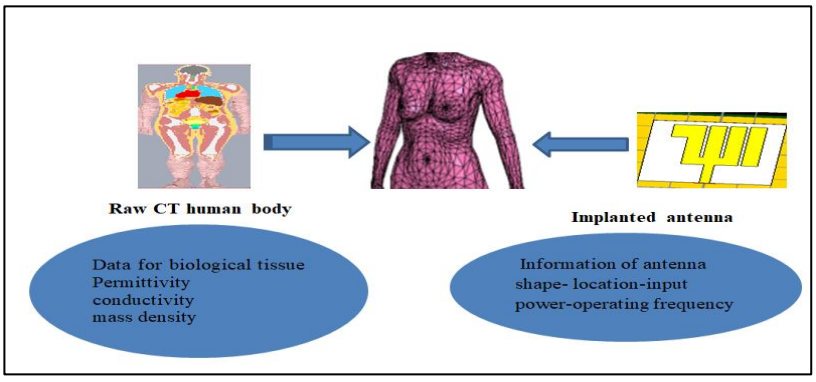

Figure 6: Schematic diagram for FIT input file generation [1]

2.5 Phantoms

2.5.1 Brain phantom

The wireless communication system in a human body, is based on the evaluation of the interactions between the human body and the electromagnetic waves radiated from the devices in the system. Phantoms have similar properties of the human body. Numerical or experimental phantoms are usually used instead of a real human body. Tissue equivalent electrical and magnetic features are used for investigations, diagnosis of different diseases. Different examples of phantoms are presented and the breast phantom of interest is explained in details at the end of the chapter.

Breast phantoms of different samples can be formed in a shape of disc composed of randomly mixed jelly, sugar and water. The electrical parameters of the tissues are available in the literature [19].

2.5.2 Torso Phantom

There are two types of torso phantoms, active and passive. For both of them, the torso is filled with a NaCl solution having conductivities of 0.16 and 0.1 S/m for active and passive ones respectively. Table1 illustrates electrical parameters of biological tissues used for the human body model at 402 MHz.

Table 1: Electrical data of biological tissues for the human body model at 402 MHZ

Biological Tissue	**Relative Permittivity** (ε_r)	**Conductivity** (σ, S/m)	**Mass Density** (g/cm^3)
Brain	49.7	0.59	1.04
Cerebrospinal fluid	71.0	2.25	1.01
Dura	46.7	0.83	1.01
Bone	13.1	0.09	1.81
Fat	11.6	0.08	0.92
Skin	46.7	0.69	1.01
Skull	17.8	0.16	1.81
Spinal Cord	35.4	0.45	1.04
Muscle	58.8	0.84	1.04
Blood	64.2	1.35	1.06
Bone Marrow	5.67	0.03	1.06
Trachea	44.2	0.64	1.10
Cartilage	45.4	0.59	1.10
Jaw Bone	22.4	0.23	1.85
Cerebellum	55.9	1.03	1.05
Tongue	57.7	0.77	1.05
Mouth Cavity	1.0	0.00	0.00
Eye Tissue	57.7	1.00	1.17
Lens	48.1	0.67	1.05
Teeth	22.4	0.23	1.85
Lungs	54.6	0.68	1.05
Heart	66.0	0.97	1.05
Liver	51.2	0.65	1.05
Kidney	66.4	1.10	1.05
Stomach	67.5	1.00	1.05
Colon	66.1	1.90	1.05
Thyroid	61.5	0.88	1.05
Spleen	63.2	1.03	1.05
Bladder	19.8	0.33	1.05

Table 2: Electrical data of biological tissues used for the human body model at 2.4 and 2.5 GHz

Body Tissue	Frequency 2.4 GHz			Frequency 2.5 GHz		
	Relative Permittivity	Conductivity (S/m)	Loss Tangent	Relative Permittivity	Conductivity (S/m)	Loss Tangent
Cartilage	38.879	1.717	0.331	38.664	1.795	0.334
Dura	42.099	1.639	0.292	41.971	1.698	0.291
Fat	5.285	0.102	0.145	5.275	0.107	0.145
Fat Mean	10.836	0.261		10.805	0.275	
G. Matter	48.994	1.773	0.271	48.830	1.843	0.271
Heart	54.918	2.216	0.302	54.711	2.297	0.302
Kidney	52.857	2.390	0.339	52.631	2.470	0.337
Liver	43.118	1.653	0.287	42.952	1.720	0.288
Lung (Inflated)	20.5	0.790	0.289	20.444	0.818	0.288
Muscle (PF)	54.487	1.844		54.348	1.920	
Muscle (TF)	52.791	1.705	0.242	52.668	1.773	0.242
Skin Dry	38.063	1.441	0.284	37.952	1.488	0.281
Skin Wet	42.923	1.562	0.272	42.783	1.622	0.272

2.5.3 Breast Phantom

It consists of fat, skin, tumor, and blood with very similar shape of the real breast. The steps of developing this phantom are summarized in [20] with the shape depicted in Figure 7 and the percentage of the materials used in the breast phantom tissue are illustrated in Table 3.

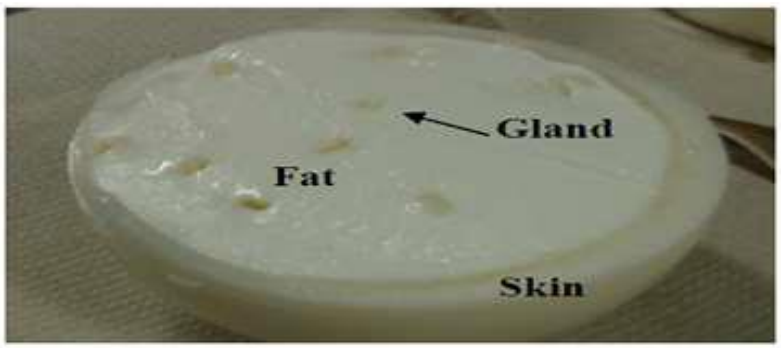

Figure 7: Hemispherical model cross-section [20]

Table 3: Percentage of material in breast phantom tissue

	Volume of Oil	p-toluic acid	n-propanol	Water	Gelatin	Formald	Oil	Surfactant
Tumor	10	0.078	3.140	74.647	13.357	0.313	7.689	0.711
Skin	20	0.070	2.802	66.619	11.921	0.280	17.160	1.095
Gland	35	0.057	2.296	54.576	9.767	0.229	31.367	1.672
Fat	80	0.017	0.815	15.565	2.789	0.066	67.996	12.753

2.6 Types of Implanted Antennas

Many challenges can be faced when designing an implantable antenna to be used within the complicated, lossy environment of the human body. Implanted antennas must be compact in size, efficient, safe, and can effectively work within adequate medical frequency bands. Working in a suitable biomedical band requires an efficient, compact antenna that fits the part of the human body that the implant device will be used. It is an urge that an implant to be used is capable of allowing transmission of data taking into account the attenuation due to lossy property of the human body which causes reduction in the efficiency. When designing a biomedical antenna, one must consider the properties of the human body which is composed of multiple layers having different electrical characteristics.

1) Simple Wire Antennas

   Simple wire antennas, dipoles and loops, can be used as implant antennas.

2) Planar Antennas

   Compact, lightweight planar antennas are designed and constructed for implant purposes. These may include meandered PIFA or spiral PIFA antennas.

Chapter 3

PRINTED PATCH ANTENNAS

3.1 Introduction

This chapter is devoted to outline the design equations and method of analysis of printed rectangular microstrip patch antennas. Transmission line and cavity model are summarized to emphasize the operation principle and the radiation mechanism of these antennas. In the following chapters, a printed antenna design will be presented. The antenna is designed and optimized based on the printed antenna principles also adopted and optimized for resonating in ISM band to be used for cancer detection.

3.2 Definition of Microstrip Antenna

In modern and recent applications, it is demanded to design and fabricate antennas which can be compatible with the needs and in the same time achieve the required performance depending on the operation and the physical function of the system in need to that antennas. Space vehicles, aircrafts, missiles, satellite, mobile and wireless communication systems acquire light weights, compact, high performance, ease of installation antennas in addition to aerodynamic profile constraint imposed in this type of systems. Microstrip antennas [21] can be a good candidate of antenna types for these applications. In recent years, the application of such type of printed antennas for diagnosis of diseases in biotechnology application is a hot point of research [5-17].

3.2.1 Advantages of Microstrip Antennas

The aforementioned features of the printed antennas in industry helps mounting antennas on the surfaces in either planar or non-planar profiles of the space vehicles and also using the MMIC design. These antennas can be designed for specific applications and optimized to active antenna parameters like gain, directivity, efficiency, polarization or impedance matching.

3.2.2 Disadvantages of Microstrip Antenna

Since the microstrip antenna comprises dielectric sandwich between the ground plane and the radiator element, is will conduct low handling power capability, high quality factor, spurious radiation from the feeder, poor scanning mechanism, higher cross polar level and very narrow band width.

3.3 Basic Construction

Basically, microstrip patch antenna depicted in Figure 8(a), is composed of a thin metallic strip patch of different configurations. The patch is implemented on a dielectric substrate mounted on a ground plane which radiates in the broadside direction. Depending on the types of feed, the excitation mode can be controlled to get an end fire patch radiator.

3.4 Feeding of Microstrip Antenna

Microstrip antenna can be fed using different configurations including coaxial probe, microstrip line, proximity coupling, aperture coupling and others [1]. Figure 8 illustrates the microstrip patch antenna feed with microstrip line and a coaxial probe. The microstrip feed line contains the copper strip, which gives a convenient characteristic impedance depending on its width. Matching the SMA connector of 50 Ohm microstrip line can be carried out using different technologies including quarter wave transformer or the inset feed. The substrate thickness also plays a very

important role in determining the impedance of the microstrip. On the other hand, the coaxial feed is also simple to be connected to the radiator via a hole in the ground plane with diameter larger than the diameter of the inner probe to avoid shorting the SMA connector. Each feeding system has advantages and disadvantages which are basically mentioned in literature [21]. In this work microstrip line feed is adopted to the antenna designed for cancer detection. The microstrip feed depicted in Figure 8 is associated with the inset feed matching technique.

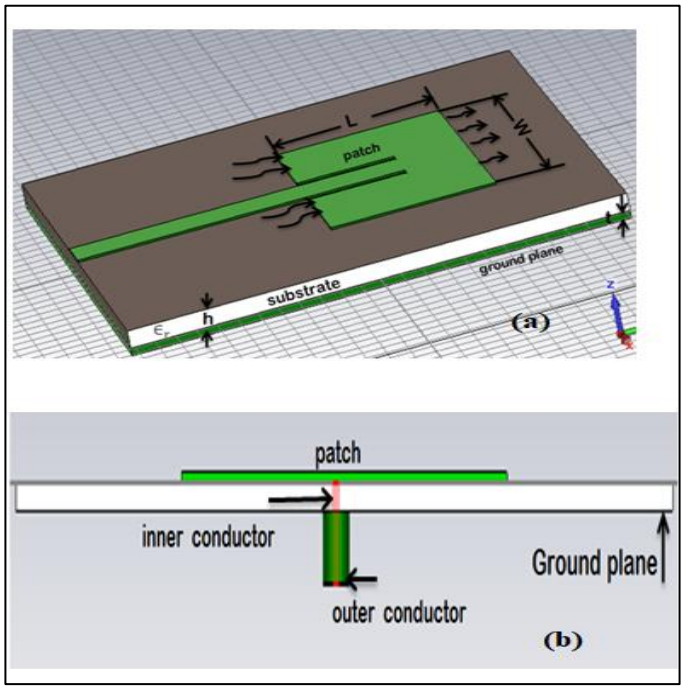

Figure 8: Some typical methods of feeding printed microstrip patch antenna.
(a) Microstrip line feed, (b) Coaxial line feed

3.5 Method of Analysis

3.5.1 Transmission Line Method

The printed rectangular antenna is considered as two openings in the form of rectangular slots separated by the length of the antenna. Slot dimensions are the width of the patch and the thickness of the substrate material. The transmission line model deals with the antenna structure as a transmission line of length equal to the

patch length with two opening ends of the patch. The edges of the printed rectangular antenna provide fringing due its finite size. Figure 9 represents the patch antenna showing the fringing effect in Figure 9(b), while Figure 9(c) illustrates the equivalent dielectric constant due to fringing effect along the slot width which can be seen along the patch length. The resonance frequency of the patch is affected by fringing, so one cannot eliminate this effect in patch antenna analysis. It can be noticed that the fringing effect makes the antenna looks wider and, in this case, makes the microstrip line look wider and longer electrically compared to its physical dimensions. Also, because the wave can be transmitted in substrate and open in air, the effective dielectric constant ε_{reff} is defined to take into consideration the fringing effect which is less than the relative permittivity of the substrate.

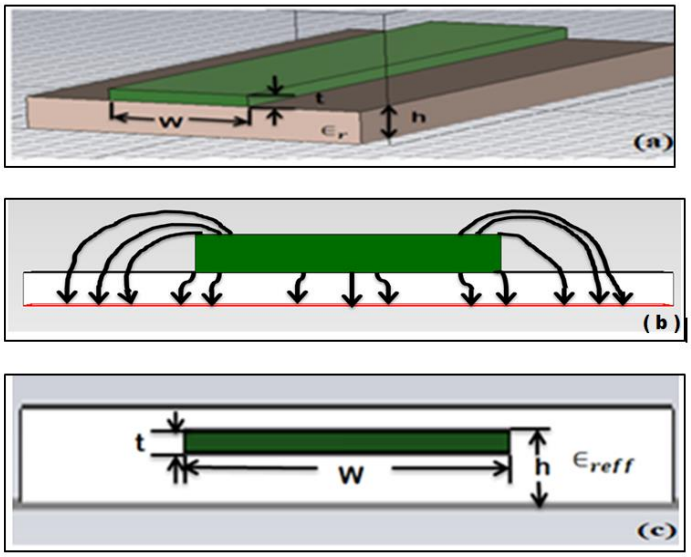

Figure 9: Microstrip line and its electric field lines, and effective dielectric constant geometry. (a) Microstrip patch, (b) Electrical field lines, (c) Effective dielectric constant

One should point out that the effective dielectric constant is frequency dependent as shown in Figure 10. The figure shows the variation of the effective dielectric

constant with the frequency for three different substrates. The values of ε_{reff} are given by $\frac{W}{h}>1$ for different types of the substrates as shown in Figure 10.

$$\epsilon_{reff}=\frac{\epsilon_r+1}{2}+\frac{\epsilon_r-1}{2}\left[1+12\frac{h}{W}\right]^{-1/2} \tag{3.1}$$

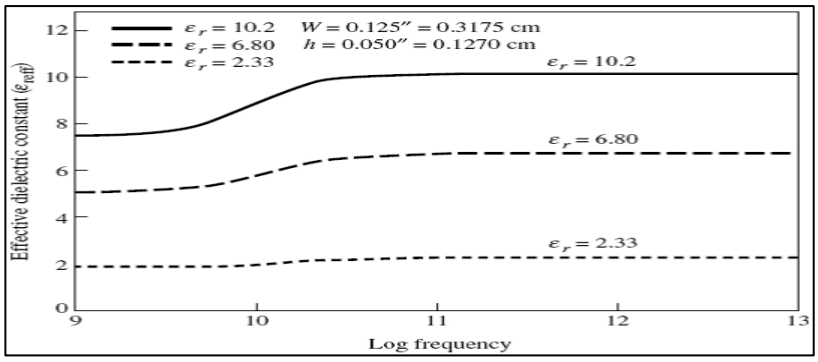

Figure 10: Different substrates with different ε_{reff} versus frequency [21]

Figure 11(a) shows the effect of fringing on the patch length, where the length is extended in both sides by ΔL, which is a function of the effective dielectric constant ε_{reff} and the ratio of width to substrate thickness (W/h). The normalized extension length is written as:

$$\frac{\Delta l}{h}=0.412\frac{(\epsilon_{reff}+0.3)\left(\frac{W}{h}+0.264\right)}{(\epsilon_{reff}-0.3)\left(\frac{W}{h}+0.8\right)} \tag{3.2}$$

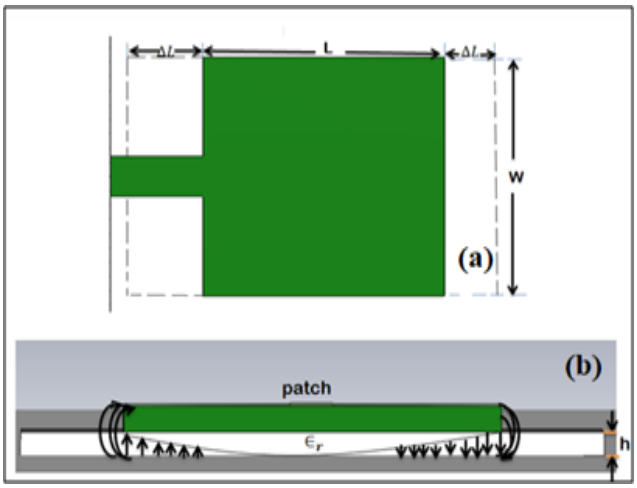

Figure 11: Physical and effective lengths of rectangular microstrip patch.
(a) Top view, (b) Side view

The total length of the patch or the effective length can be written as

$$L_{eff} = L \tag{3.3}$$

where L = λ/2 is the length of the patch for dominant TM_{010} mode with no fringing [21]. Also the resonance frequency of that dominant mode is:

$$(f_r)_{010} = \frac{1}{2L\sqrt{\epsilon_r}\sqrt{\mu_0\epsilon_0}} = \frac{C_0}{2L\sqrt{\epsilon_r}} \tag{3.4}$$

Taking the fringing into account,

$$(f_{rc})_{010} = \frac{1}{2L_{eff}\sqrt{\epsilon_{reff}}\sqrt{\mu_0\epsilon_0}} = \frac{1}{(2L+2\Delta L)\sqrt{\epsilon_{reff}}\sqrt{\mu_0\epsilon_0}}$$
$$= q\frac{1}{2L\sqrt{\epsilon_r}\sqrt{\mu_0\epsilon_0}} = q\frac{C_0}{2L\sqrt{\epsilon_r}} \tag{3.5}$$

where,

$$q = \frac{(f_{rc})_{010}}{(f_r)_{010}} \tag{3.6}$$

The q factor is the fringe factor (length reduction factor). Increasing the substrate height will increase the fringing and hence enlarge separations between the slots and as a result decreases the resonant frequency.

Rectangular Patch Input Resistance

Since the rectangular patch length is approximately half wave length, then one can make a transformation of the output admittance to the input terminal by a length of half wavelength. For the sake of matching to the source using the inset fed technique shown in Figure 12(a), the following equation is hold .In Figure 12(b) the radiating slot is represented with a parallel equivalent admittance slot 1, $Y_1 = G_1 + jGB_1$, slot 2, $Y_2 = G_2 + jGB_2$,where E_1 is the electric field radiated by slot 1, H_2 is the magnetic field radiated by slot 2, V_0 is the voltage across the slot and the sign is termed for the odd mode and even mode of the voltage under the printed rectangular patch

antenna,and Figure 13 shows the impedance versus y_o , the strip width, it results in the antenna input impedance of:

$$Z_{in} = \frac{1}{Y_{in}} = R_{in} = \frac{1}{2G_1} \tag{3.7}$$

Taking the coupling effect between the slot into account, the impedance is modified to be:

$$R_{in} = \frac{1}{2(G_1 \pm G_{12})} \tag{3.8}$$

where conductance $G_1 = \begin{cases} \frac{1}{90}\left(\frac{W}{\lambda_0}\right)^2 & W << \lambda_0 \\ \frac{1}{120}\left(\frac{W}{\lambda_0}\right) & W >> \lambda_0 \end{cases}$

and mutual conductance $G_{12} = \frac{1}{|V_0|^2} Re \iint (E_1 \; X \; H_2^*) \, . ds$

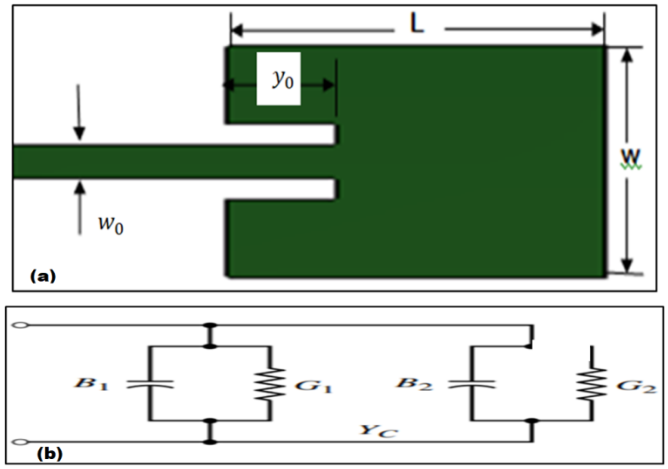

Figure 12: (a) Inset feed technique for rectangular patch,
(b) Transmission model equivalent

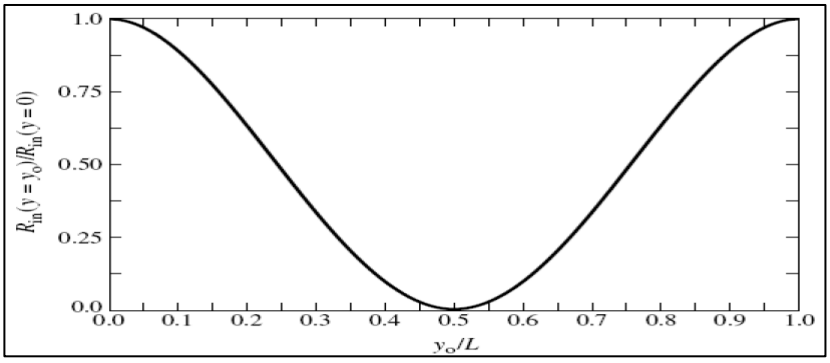

Figure 13: The normalized impedance as a function of y_o [21]

Characteristic impedance is given by:

$$Z_c = \begin{cases} \frac{60}{\sqrt{\epsilon_{reff}}} \ln\left[\frac{8h}{W_0} + \frac{W_0}{4h}\right] \frac{W_0}{h} & \leq 1 \\ \frac{120\pi}{\sqrt{\epsilon_{reff}}\left[\frac{W_0}{h} + 1.393 + 0.667 \ln\left(\frac{W_0}{h} + 1.444\right)\right]} \frac{W_0}{h} & > 1 \end{cases} \quad (3.9)$$

The input resistance for the inset feed:

$$R_{in}(y = y_0) =$$

$$\frac{1}{2(G_1 \pm G_{12})} \left[\cos^2\left(\frac{\pi}{L} y_0\right) + \frac{G_1^2 + B_1^2}{Y_c^2} \sin^2\left(\frac{\pi}{L} y_0\right) - \frac{B_1}{Y_C} sin\left(\frac{2\pi}{L} y_0\right)\right] \quad (3.10)$$

where, $Y_c = \frac{1}{Z_c}$, since for most typical microstrip lines: $G_1/Y_c \ll 1$ and $B_1/Y_c \ll 1$. The equation reduces to:

$$R_{in}(y = y_0) = \frac{1}{2(G_1 \pm G_{12})} \cos^2\left(\frac{\pi}{L} y_0\right)$$

$$= R_{in}(y = 0) \cos^2\left(\frac{\pi}{L} y_0\right) \quad (3.11)$$

Chapter 4

STAGE I CANCER DETECTION IN HUMAN BREAST USING BIOLOGICAL AND ELECTROMAGNETIC PROPERTIES OF BREAST TISSUES

4.1 Introduction

Recently, academic and technical development in bioengineering and science is a point of interest for the sake of reducing the need for invasive surgical operations and for constant health monitoring, hence the demand of implant antennas on human body for diagnosis and treatment procedure are urgent and need more attention. On the other hand implantable antennas can be considered as a main building element in communication network between doctors/hospital and patients in (ISM) frequency band [1-27]. Implanted antenna should be compact, lightweight and low cost. Also should have a secure frequency band to operate on and not be harmful for human tissues. The ISM band systems can transmit information from antenna on/in a body to outside through a wireless communication system [28].

According to American Joint Committee on Cancer (AJCC), breast cancer is classified into stages according to the size and location of tumors. In stage 1A, the size of the tumor varies from 0.5 up to 2 cm and it is considered to be spread on breast, whereas stage 1B has either tumor of same size in breast associated with

group of tumors in lymph nodes of size from 0.2mm up to 2mm or tumors only in lymph nodes.

This chapter is illustrating cancer detection in breast by using the biological and electromagnetic properties of breast tissues for stage 1 cancer. An antenna placed on the breast surface is used for this purpose. This antenna, is made of copper annealed conductor implemented on FR4 substrate with relative dielectric constant 4.3, thickness 1.6mm, loss tangent 0.025 and is operating on industrial, scientific, and medical (ISM) frequency band. The ground is truncated to tune the antenna in this frequency band. The multilayer breast structure is modeled as three parallel layers of skin, fat, and glandular. On the other hand a model including additional lymph nodes is also presented. Return loss results are used for studying the effect of normal and infected beast tissues. Different sizes and number of tumors are tackled to visualize the presence of the first stage of cancer disease. The adapted antenna is fabricated and return loss results are measured by using a network analyzer which is celebrated using open circuit, short circuit and match load terminations before doing any measurement for return loss. The results are obtained on free space and on normal human breast. The simulations of different structures are carried out on CST microwave studio. There is a fair agreement between the measured and simulated results. The applied scenario gives a future proposal for some element bricks to build a communication link for breast cancer detection and to reduce the need for invasive surgical operations. It is also feasible to be applied in the intermediate steps during treatment. The study of this chapter, is devoted to both stages 1A and 1B.

4.2 Antenna Design

Figure 14 depicts the printed antenna [3] which consists of different bricks of copper annealed and implemented on FR4 substrate with relative dielectric constant of 4.3, thickness of 1.6mm and loss tangent of 0.025. The dimensions of the antenna are 5x4 cm^2 and is fed with a microstrip line of 50 Ω. The fabricated antenna is illustrated in Figure 15 and the dimensions of the structure are given in Table 4. The optimization details of the design is given in Appendix A. Figure 14 depicts the printed antenna [3] which consists of different bricks of copper annealed and implemented on FR4 substrate with relative dielectric constant of 4.3, thickness of 1.6mm and loss tangent of 0.025. The dimensions of the antenna are 5x4 cm^2 and is fed with a microstrip line of 50 Ω. The fabricated antenna is illustrated in Figure 15 and the dimensions of the structure are given in Table 4. The optimization details of the design is given in Appendix A.

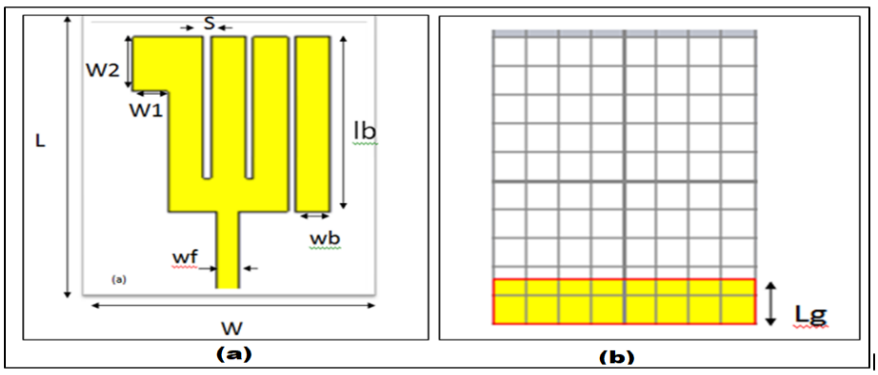

Figure 14: Antenna design. (a) Top view, (b) Bottom view

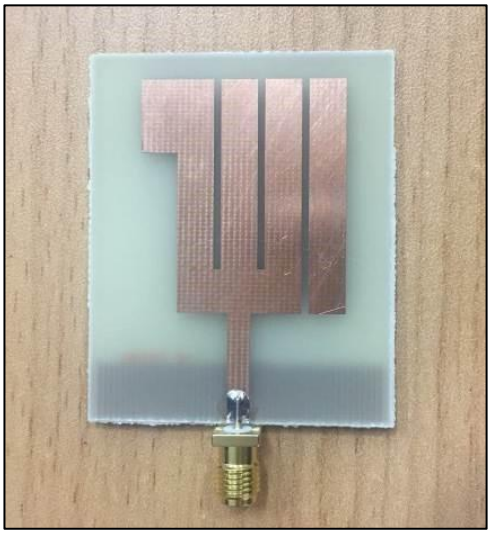

Figure 15: Fabricated antenna

Table 4: Antenna Dimensions

Parameter	Dimension in mm
Height of the Substrate	1.6
L	50
W	40
Lb	32
Wb	5
W1	5
W2	10
Wf	3.11
Lg	8
S	1

Figure16, shows the E and H plane far field radiation patterns of the antenna in free space.

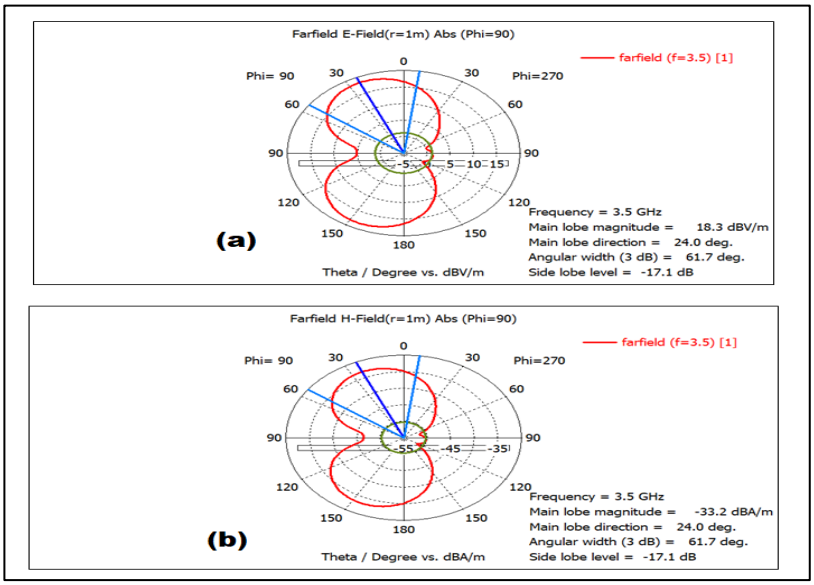

Figure 16: E and H plane far field radiation pattern. (a) E field, (b) H field

4.3 Biological Models

The effect of the tumorous cells in the breast, on the return loss is investigated by considering the simplest human breast model made of skin only shown in Figure 17 and then the biological literature is followed for real breast cancer stage models [29].

Series simulations are carried out by placing the antenna on simple single and multilayer breast models to investigate the return loss behavior of the antenna when placed on breast models.

The fields radiated by the antenna placed on the breast are reflected back due to the difference in the impedances of free space, the breast and the antenna input impedance. These reflections are monitored by using the return loss parameter S11.

When the intrinsic impedances of layers change, the input impedance of the antenna further changes and thus the reflection (S11) at the input terminal changes.

The tumorous tissues within different layers of the breast, further change the return loss at the antenna input terminal because of higher dielectric constants and conductivities. Obviously, the difference in the constitutive parameters of breast, changes the return loss compared with the normal breast especially when the tumor sizes are significant.

A simple breast model as shown in Figure 17 is considered to demonstrate the variation of the return loss of different size malignant tissues. The return loss curves of the normal and the tumorous breast models possessing different dimensions are compared. Any difference in the return loss may be a sign of cancerous tumor and needs further investigation by consultants/doctors.

Figure 18 illustrates the return loss results of three different simulations, each time having tumors with different dimensions and placed close to the antenna surface. The radii of each tumor are 1.5cm, 3cm, 5cm and the depth is taken constant as1cm for all cases. The upper surface of the tumor is placed at the center of the breast layer and placed 5.8 mm below the breast surface. Figure 18 shows about 6 dB difference in the return loss of 5cm tumor and the normal breast which is the indication of a structure with higher dielectric constant cells in that region, i.e., the tumor.

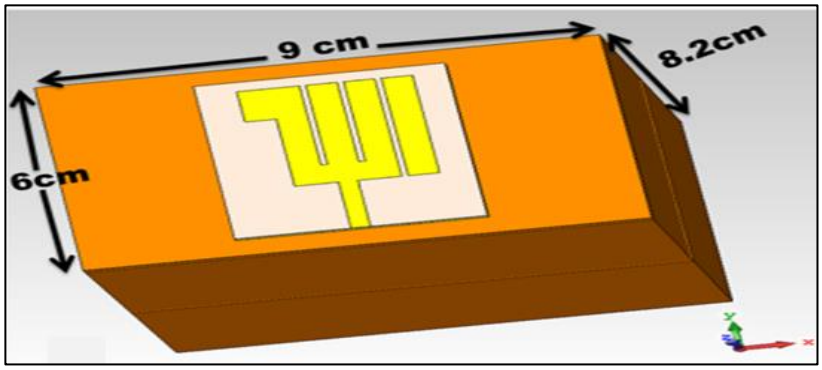

Figure 17: Breast model composed of skin layer

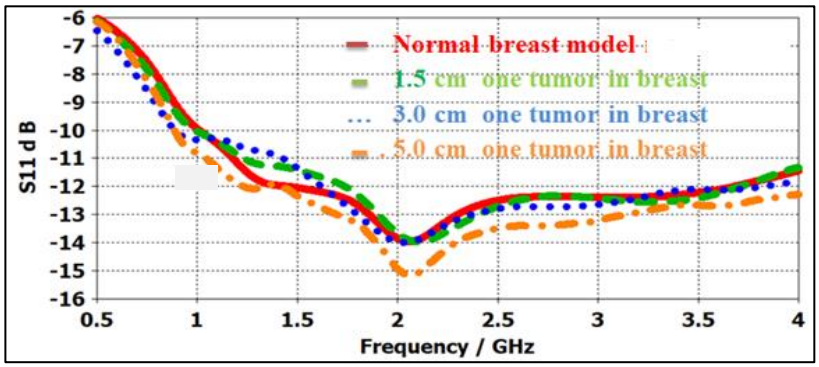

Figure 18: Simulated return loss for 1 tumor cell in breast

When the body acts as a communication channel for the propagation of the electromagnetic waves, attenuations take place due to the abortion of the power in a lossy medium. Radiated fields by the antenna will penetrate and the tumors in deep regions of the human breast may not be detected. This phenomenon may be overcome by using lower frequency signals for the simulations. Figure 19 illustrates the results of the similar scenario, except replacing the tumors in the deeper region of the breast at 38.4 mm below the breast surface, again in the skin layer. This simulation study shows the effects of the lossy dielectric properties of the human body tissue in the signal strength.

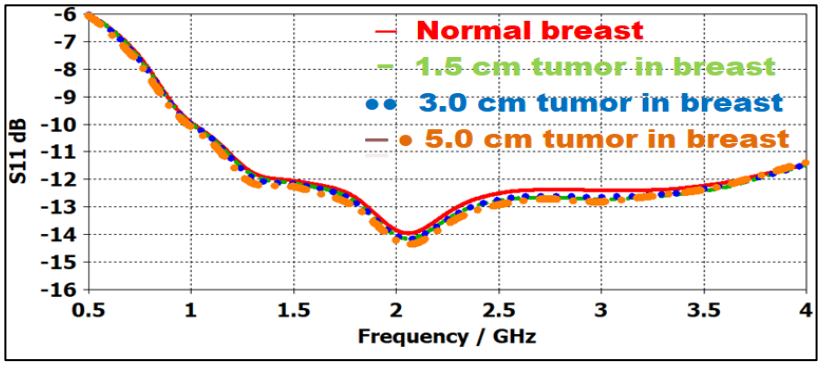

Figure 19: Simulated return loss for 1 tumor cell in breast

4.4 Breast Model

The human breast composed of multilayers is modeled as shown in Figure 20. In Figure 20(a) the breast is illustrated without lymph nodes. It consists of three layers; skin, fat and glandular with relative dielectric constants and electrical conductivities of 38, 1.46, 5.15 0.138, 57.2 and 1.9 respectively. Figure 20 (b) represents the breast associated with the lymph nodes. The lymph layers are skin, fat and muscles with relative dielectric constants and electrical conductivities of 38.006, 1.464, 5.28, 0.105, 53.75 and 1.81. The relative dielectric constant and electrical conductivity of the lymph node itself is 78 and 0.965 respectively. The missing dimensions of both structures are shown in Table 5.

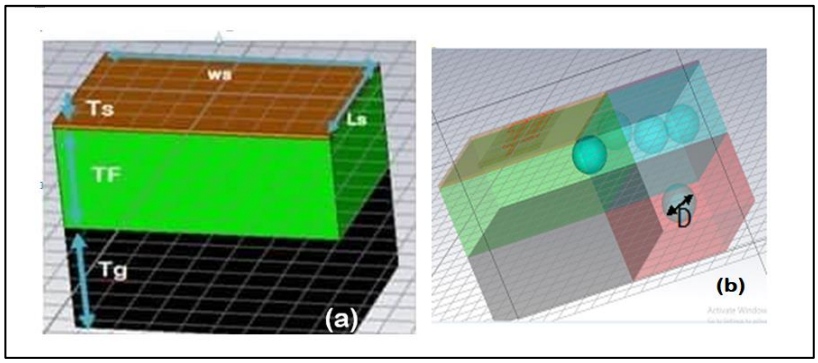

Figure 20: Breast model: (a) The multilayer breast model,
(b) The beast model with lymph node

Table 5: Antenna dimensions breast model dimensions

Parameter	Dimension in mm
WS	90
Ls	60
Ts	2
Tf	40
Tg	40
D	20

4.5 Simulation and Measured Results

To study the effect of tumorous tissues on the return loss of the antenna for infected human breast, the antenna is placed on the breast model as illustrated in Figure 21. In Figure 21 (a) the antenna is on the breast without lymph nodes, while in Figure 21 (b) it is placed on the breast with lymph node structure. Both cases are simulated by using CST Microwave Studio.

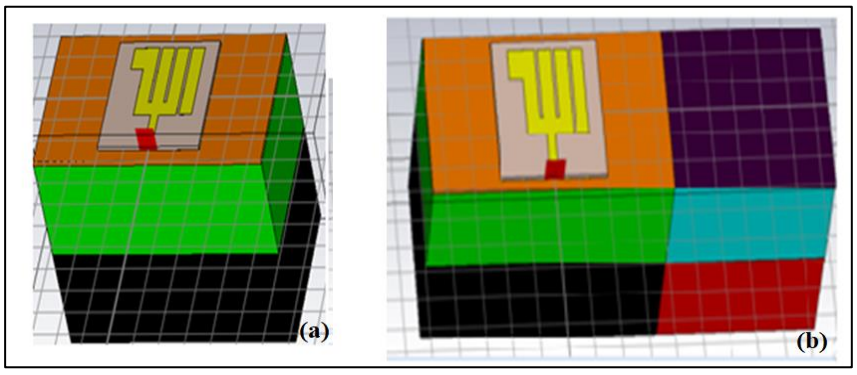

Figure 21: Antenna on breast model. (a) On breast,
(b) On breast with lymph nodes

The simulated and measured return loss of the adapted antenna in free space (without breast) is shown in Figure 22. The measurement is carried out on the antenna in free space by using network analyzer Rohde & Schwarz ZWB20. The antenna resonates

at higher frequency 3.5 GHz with gain and directivity 3.84 dB, 4.08 dB respectively. One notices some differences between the simulated and measured results which confirm the design and assessment procedures. It is very important to point out that these return losses are the results of the breast without tumors. This is taken as a reference for all cases to investigate the effect of tumors on the antenna performance for two distinct cases, with and without lymph nodes.

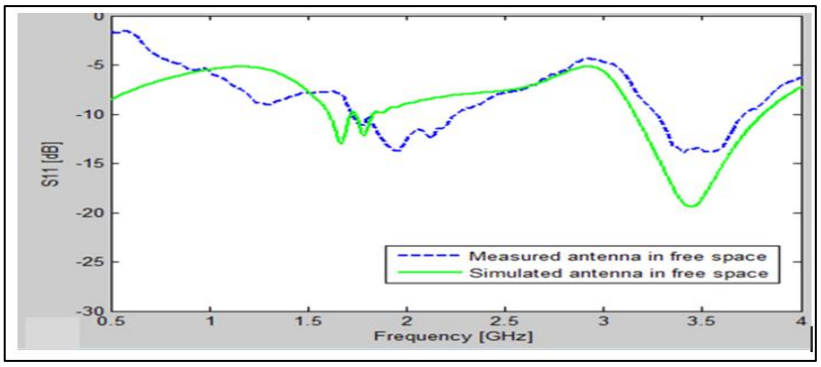

Figure 22: Simulated and measured return loss of antenna in free space

Figure 23 depicts the simulated and measured return loss results of the antenna placed on the breast with and without lymph nodes for normal body. The number of lymph nodes is chosen according to the biological literature available [29].

One notices that the antenna resonates in ISM band at 2.11GHz and 2.13GHz with directives 4.87 dB, 4.78 dB for the model without and that with lymph nodes respectively. It is also realized that the gain of the antenna is very small (-7.3 dB, -9.26 dB) since most of the power is absorbed by the human tissues of the breast.

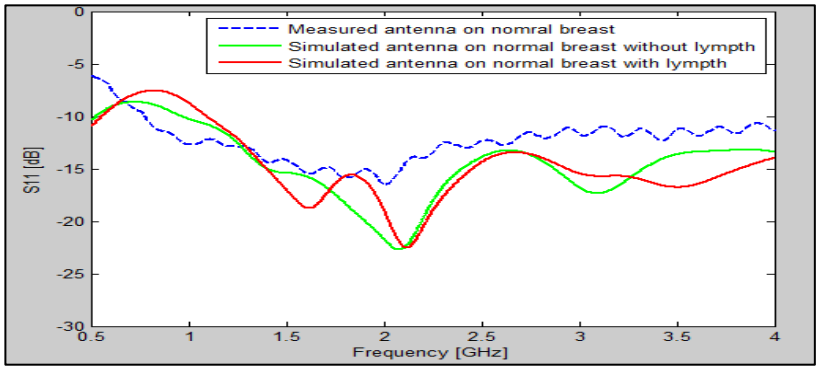

Figure 23: Simulated and measured return loss of antenna on normal breast

Although the return loss curves show similar behavior, in the frequency band of 2-4GHz maximum 5dB difference can be observed. This difference between the measured and simulated results are due to the surrounding effects of the antenna measurement under the normal laboratory conditions**.** Simulation results using high order approximations and absorbing boundary conditions on the truncation planes and experimental measurements under the anechoic chamber laboratories conditions give more reliable results compared to the analytical solutions.

Antenna placed on the breast model without lymph nodes in stage 1A with different structures and number of tumors are studied and the results are demonstrated in Figures from 24 to 32. The tumor radii are considered to be 0.5 cm, 1.0 cm, 1.5 cm and 2.0 cm. Figures from 33-35 demonstrates the simulation models.

For each value of tumor radius the tumor depth values are 1.0 cm, 2.0 cm and 3.0 cm. On the other hand different number of tumors in each layer is considered (1, 3, and 5). The return loss of normal breast is superimposed in each figure as a reference. One concludes that increase in the tumor radius either shifts the resonance frequency or changes the value of the return loss. Moreover, increasing the number of tumorous cells increases the discrepancy of the return loss.

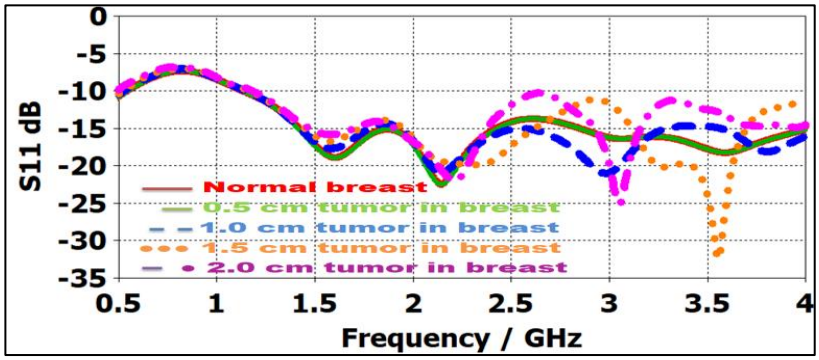

Figure 24: Simulated return loss for 1 tumor cell in each layer of breast depth 1cm

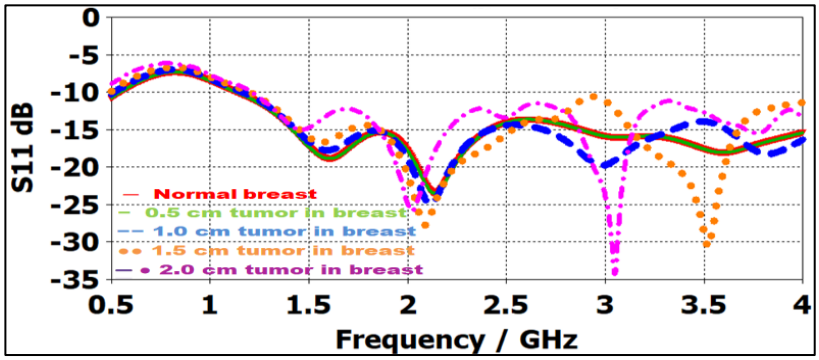

Figure 25: Simulated return loss for 3 tumors cell in each layer of breast depth 1cm

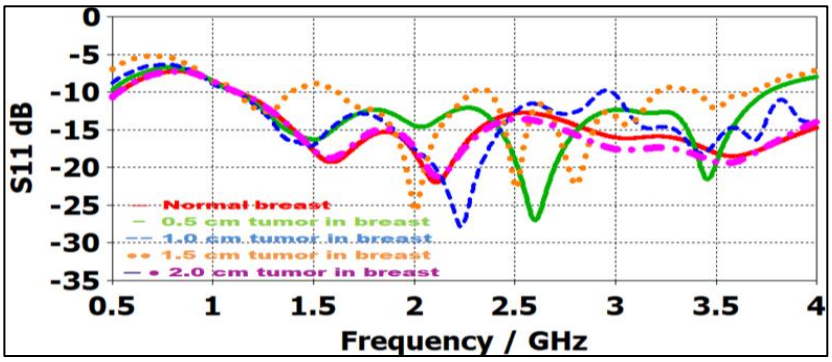

Figure 26: Simulated return loss for 5 tumors cell in each layer of breast depth 1cm

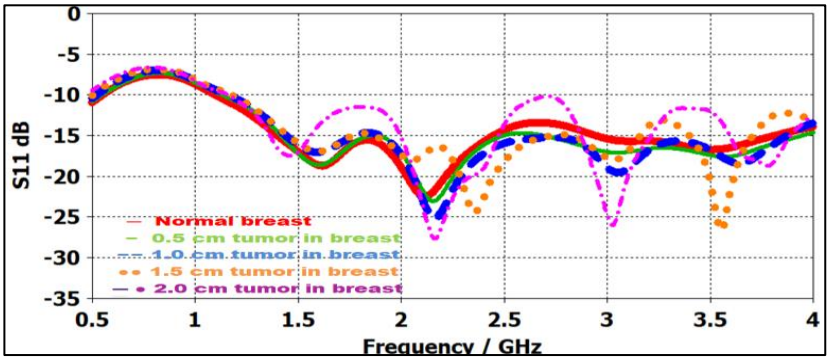

Figure 27: Simulated return loss for 1 tumor cell in each layer of breast depth 2cm

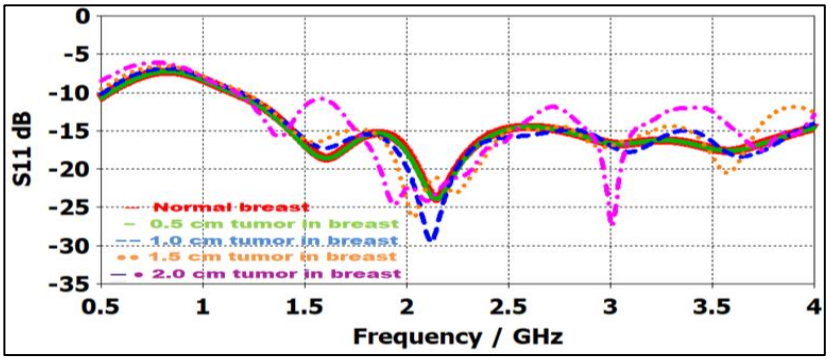

Figure 28: Simulated return loss for 3 tumor cell in each layer of breast depth 2cm

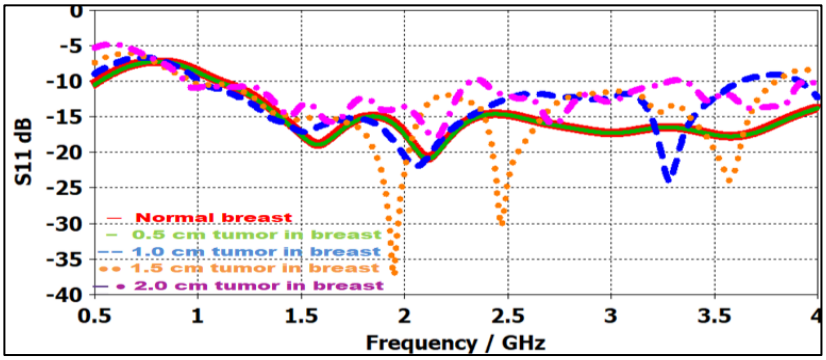

Figure 29: Simulated return loss for 5tumor cells in each layer of breast depth 2cm

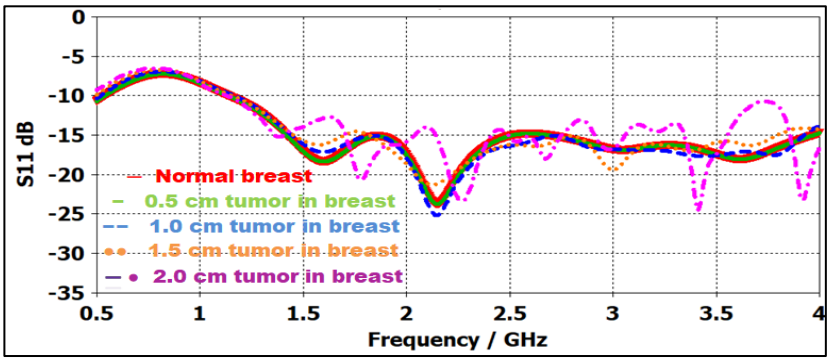

Figure 30: Simulated return loss for 1 tumor cells in each layer of breast depth 3cm

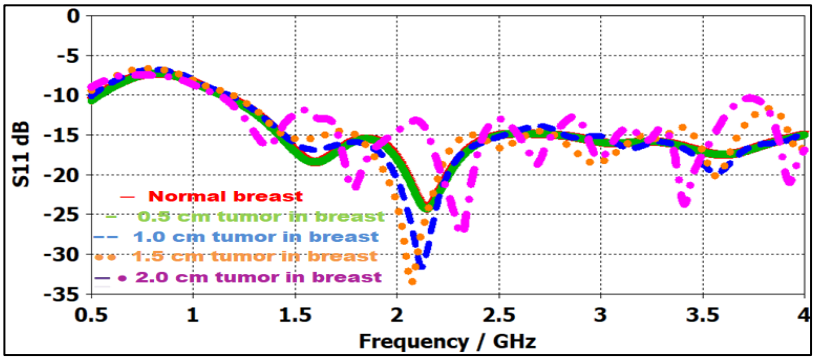

Figure 31: Simulated return loss for 3 tumor cells in each layer of breast depth 3cm

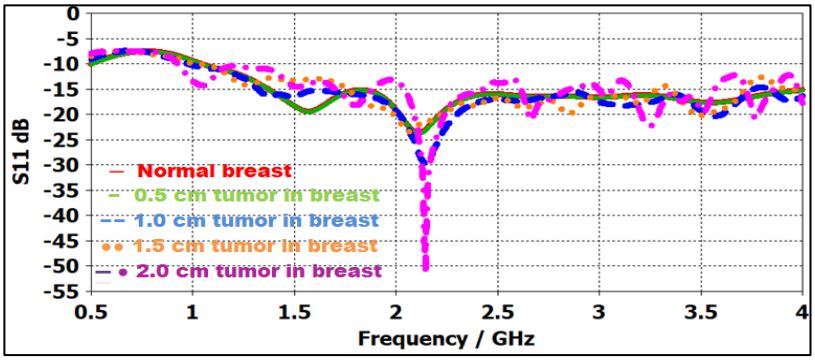

Figure 32: Simulated return loss for 5 tumors cells in each layer of breast depth 3cm

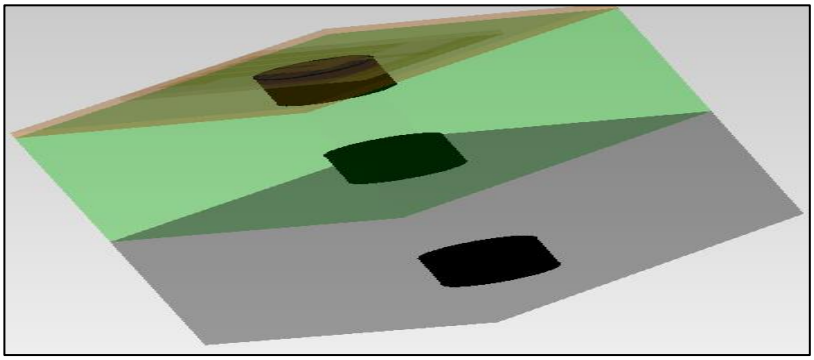

Figure 33: One tumor cell in each layer of breast

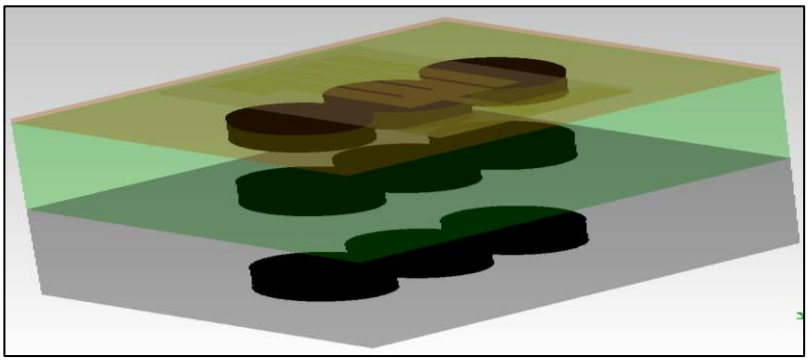

Figure 34: Three tumor cells in each layer of breast

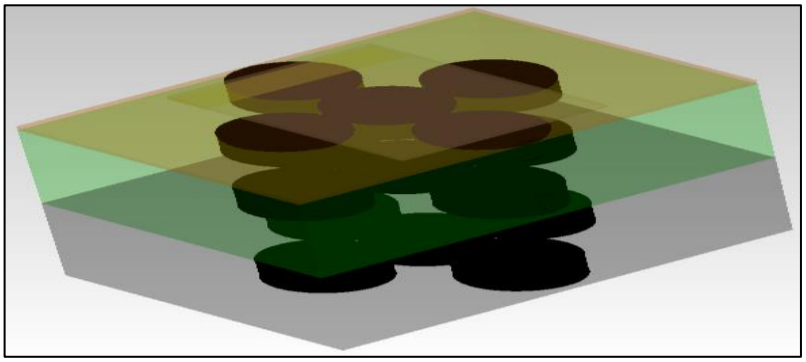

Figure 35: Five tumor cells in each layer of breast

In the study of stage 1B cancer case, an antenna is placed on a similar breast model by adding various number of lymph nodes and tumor cells of 1.9mm radii in lymph nodes. Figure 36 shows the structure of the breast model with tumors and lymph nodes with tumors. Figure 37 presents the corresponding results of one tumor cell in each layer of the breast model and one tumor in each 3 lymph nodes. It is clear that increase in the size of tumor in breast shifts the resonant frequency relative to normal breast as shown by the graphs of tumor sizes 1.5cm and 2 cm. Figure 38 shows the results of five tumor cells in breast and one tumor in each 3 lymph nodes. The return loss of normal breast is superimposed in each figure as a reference. One concludes that the span of change of the return loss variation is higher when the tumors in lymph nodes (from -5dB to -45dB, compared to -5dB to -25dB for the case without tumors in lymph) are included. This is a good indication that the adopted design is sensitive for the of the stage assessment of breast cancer.

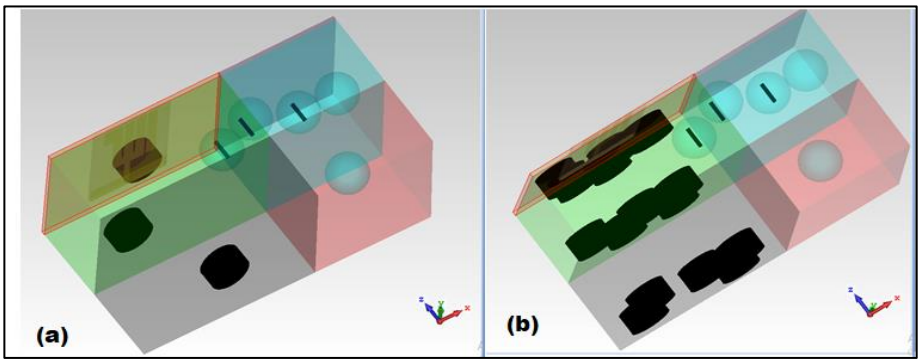

Figure 36: one and five tumors cell in each layer of breast with one tumor cell in lymph. (a) One tumor cell in each layer, (b) Five tumors cells in each layer

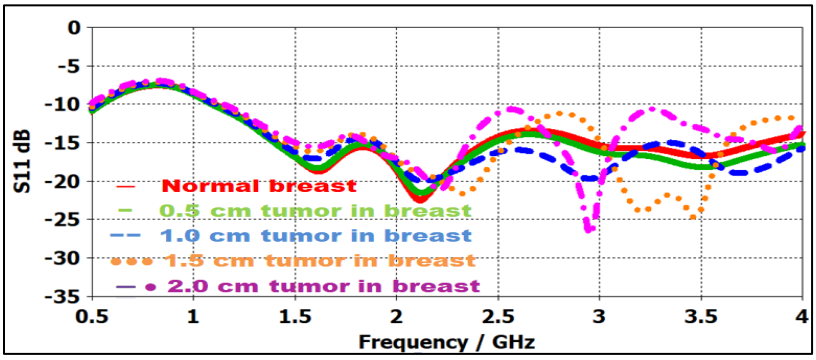

Figure 37: Simulated return loss for 1 tumor cell in each layer of breast with one tumor cell in each 3 lymph node

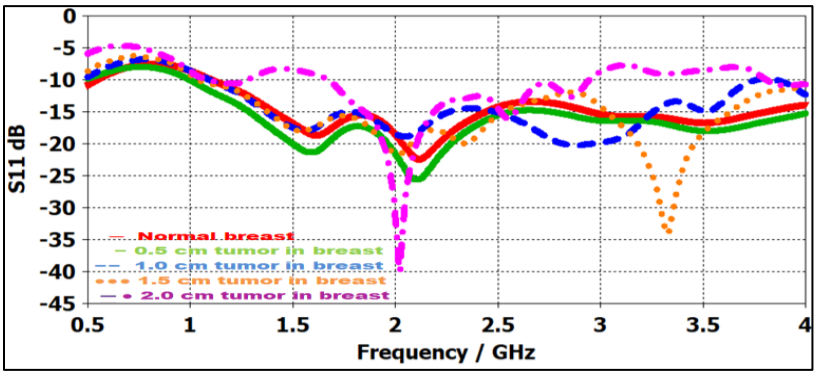

Figure 38: Simulated return loss for 5 tumor cell in each layer of breast with one tumor cell in 3 lymph nodes

For the case of stage 1B with no tumors in breast, the effect of the number of tumors in lymph nodes varying from 1 to 8 are observed. Figure 40 shows that, increasing the number of tumors in the lymph nodes, give rise to a change in the return loss results. This case is consider as the very early stage of the cancer in the body. This confirms that the scenario adopted in this work is sensitive to the tissue changes in the breast that may be the indication of the cancer in very early stages.

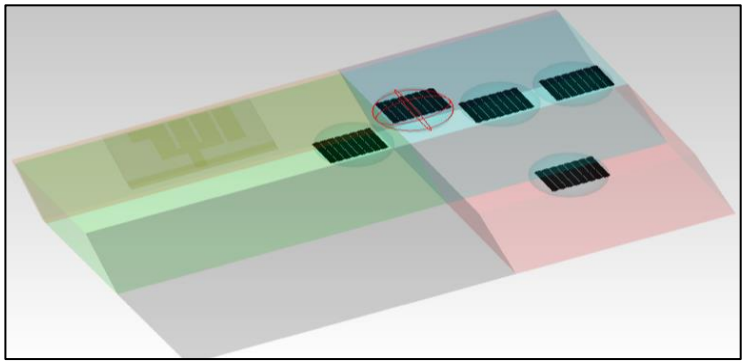

Figure 39: Tumors in lymph nodes

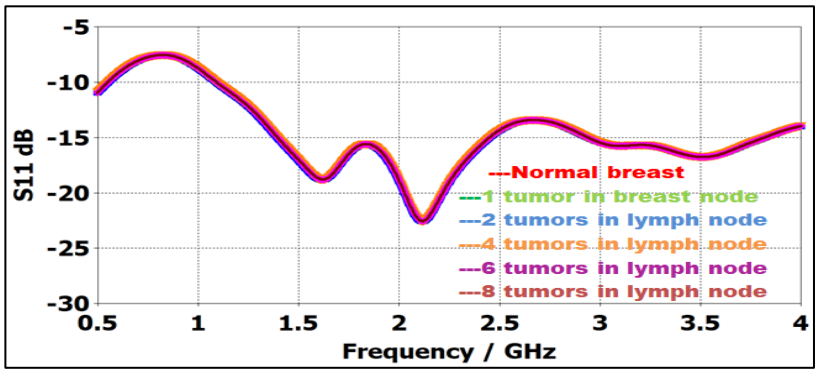

Figure 40: Simulated return loss for only tumors in lymph nodes

4.6 Conclusion

In this chapter an antenna is designed to be implanted on human breast. It is measured and simulated in free space and on a real human breast. The antenna is devoted to measure the effect of malignant tissues either in the breast or in lymph nodes, on the antenna performance concerning the return loss as the main parameter. It is concluded that, increasing the tumor radius either shifts the resonance or changes the values of the return loss. Moreover, increasing the number of tumors cells increases the discrepancy of the return loss image. On the other hand the adopted analysis can sense the case of cancer in the very early stage in the body.

Chapter 5

STAGE II CANCER DETECION USING PRINTED ANTENNA PLACED ON A HEMISPHRICAL HUMAN BREAST MODEL

5.1 Introduction

It is declared in Chapter 4 that breast cancer stages of this study are defined according to the American Joint Committee on Cancer by taking size and location of the tumors into account. According to AJCC Stage II A, is defined as follows; either (a) “No actual tumor is associated with cancerous cell in breast, a single tumor larger than 2 mm and less than 2cm is found in 1 to 3 lymph nodes under the arm or (b) multiple tumors found in the lymph nodes near the breast with size less than 2cm and none in lymph nodes under the arm”. On the other hand stage II B is define as one of following; either (a) “a small groups of breast cancer cells with size larger than 2cm but smaller than 5 cm with tumors larger than 0.2mm but not larger than 2mm are found in the lymph nodes or (b) a tumor larger than 2cm but smaller than 5cm and cancer cell spread to 1 to 3 axillary lymph nodes, or to cancer cell in lymph nodes near the breast or tumors larger than 5cm and in the breast”.

This chapter is devoted to cancer types of stage II, detection of any tumor in breast using the electromagnetic properties of electromagnetic properties of human breast as considered in Chapter 4. Deviation of the malignant cells properties from those of

standard human breast cells directly affects the performance of an antenna placed on the breast under test. In addition to the return loss, the gain, and directivity of the antenna are used as images for studying the effect of normal and infected tissues in this chapter. A new breast model is presented in this part of the study which covers the breast, part of the human skin and fats under breast and part of the human lymph nodes connected to the breast. Different sizes and number of tumors are tackled to visualize the second stage of cancer detection. Moreover spread of tumors in breast and in lymph nodes are illustrated demonstrating stage II cancer. Similarly, simulations are carried out on CST microwave Studio. There is a fair agreement between the measured and simulated results of the normal human breast and the simulation of a breast with similar dimensions. The adopted work gives a future proposal for some element bricks to build a communication link for breast cancer diagnosis and reduces the need for invasive surgical operations. It is also feasible to be applied in the intermediate steps during treatment.

The antenna adopted in this diagnosis is the same one used in the previous chapter and is shown in Figure 14, therefor the fabricated antenna is illustrated in Figure 15 and the dimensions of the antenna are depicted in Table 4.

5.2 Breast Model

Figure 41 illustrates the hemispherical simulation model of female human breast. The model comprises three main parts, firstly, a breast of three spherical shape layers; skin, fat, and glandular is presented. Secondly, the breast is associated with the lymph nodes with lymph layers; skin, fat and muscles. Thirdly, associated part of the body under breast is included. The lymph nodes are illustrated in Figure 42. The conductivity and relative dielectric constant of the different layers and lymph nodes

are shown in Table 6 while the dimensions are depicted in Table 7. The antenna is placed on top of the breast where the truncated ground is touching the top layer of the breast.

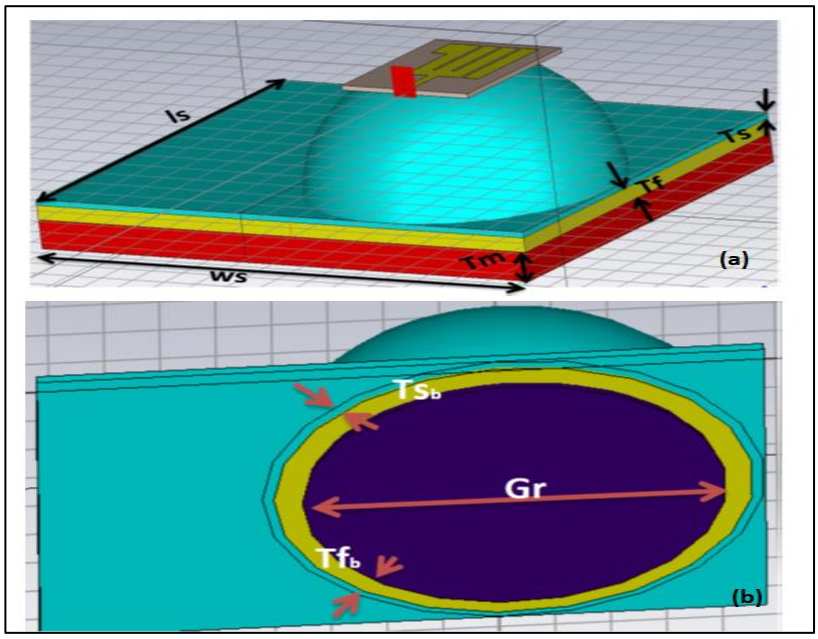

Figure 41: Breast Model. (a) Top view, (b) Bottom view

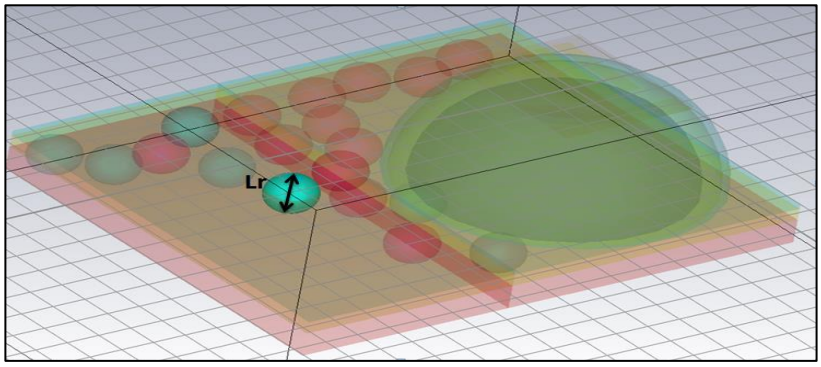

Figure 42: Breast model showing the lymph nodes inside

Table 6: Electric properties of the different layers of breast model

Material	Permittivity	conductivity
Tumors	59	0.15
Breast gland	57.2	1.97
Breast skin	38.006	1.464
Breast fat	5.14	0.137
Lymph nodes	78	0.965
Model skin	38.0006	1.464
Model fat	5.28	0.104517
Model muscle	52.7	1.810395

Table 7: Dimensions of breast model

Center Radius of skin breast, mm	Cr	90
Top radius of breast, mm	Tr	40
Glandular radius of breast, mm	Gr	76
Thickness of breast skin, mm	Tsb	2
Thickness of breast fat, mm	Tfb	5
Radius of lymph node, mm	Lr	10
Thickness of skin, mm	Ts	2
Thickness of fat, mm	Tf	5
Thickness of muscle, mm	Tm	10
Length of model, mm	Ls	130
Width of model , mm	Ws	155

5.3 Simulation and Measured Results

The return loss study of the cancerous tissues on the return loss of the antenna, is made by placing the antenna on the hemispherical breast model illustrated in Figure 41. The return loss of the antenna acting on a healthy breast is simulated using CST as before and the results are illustrated in Figure 43. Measured return loss results detected by the network analyzer are taken as reference and demonstrated on the same figure for comparison. The antenna resonates at 2.11 GHz with a directivity of

5.18 dB. It was noticed that the gain of the antenna is -14.85 dB; which is significantly low, since most of the power was absorbed by the breast tissues. These results at this point in the study, act as a reference for detection of cancerous tissues.

For the diagnosis of stage II breast cancer, many simulations are carried out to measure the return loss while varying the number of tumors and using different spreads of cylindrical shaped tumors, with relative permittivity of 59 and conductivity of 0.15 S/m [31] in the breast tissues, lymph nodes and the arm.

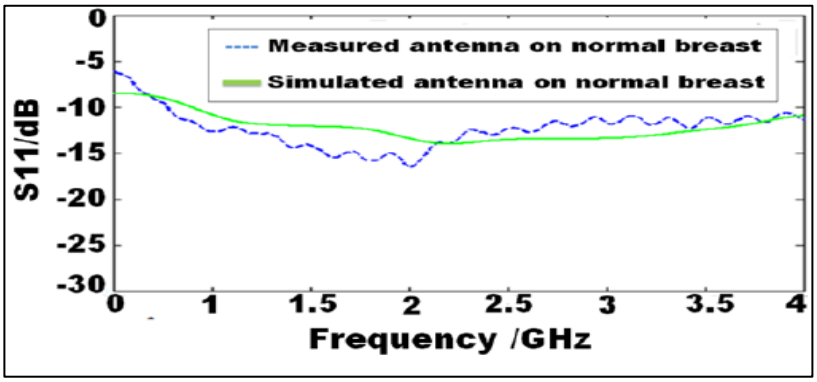

Figure 43: Simulated and measured return loss of antenna implemented on healthy breast

The study started with Case 1, with three tumors in the lymph nodes under the arm, having radii 0.5 cm, 1.0 cm, and 1.5 cm. The simulation results of the returnloss for the three different radii gave identical results as that of a healthy breast, as shown in Figure 44.

In Case 2, three tumors are placed near the breast as shown in Figure 45. The tumor radii taken are 0.5 cm, 1.0 cm, and 1.5 cm. The values of the return loss for the three different radii alongside the return loss of a healthy breast are depicted in the simulated return loss of Figure 46.

It can be noticed that the simulated return losses for Case 2 are lower than that of the normal breast by 3.5 dB but they do not dependent on the tumor size. The results indicate that as tumors approach the breast; early stage II cancer, the distinction becomes clearer.

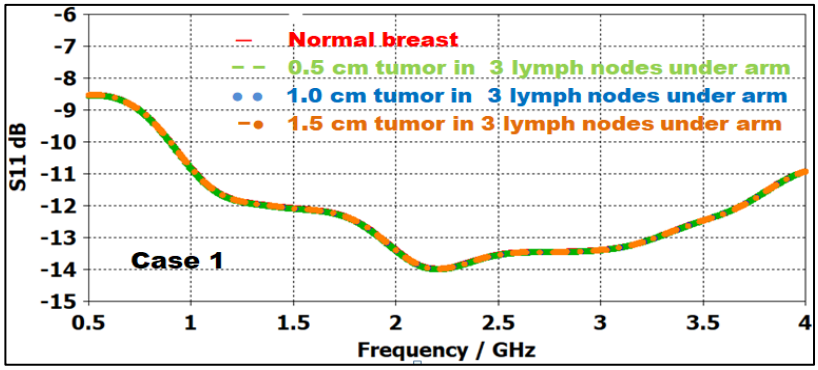

Figure 44: Simulated return loss for tumors under arm case 1

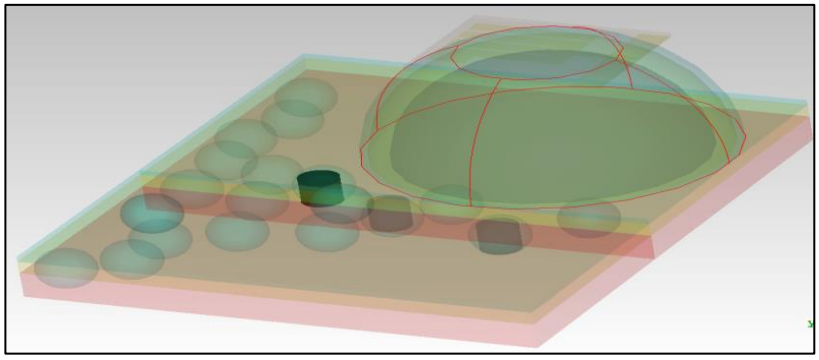
Figure 45: Three Tumors near to the breast case 2

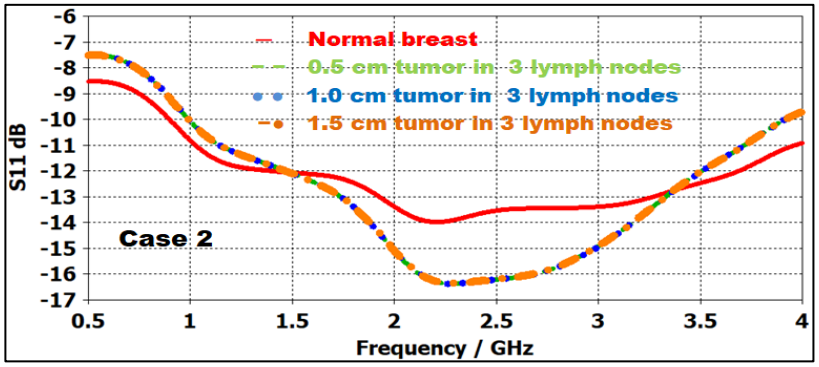

Figure 46: Simulated return loss for tumors case 2

In Case 3, three tumors are added within the breast in addition to three tumors in the lymph nodes as shown in Figure 47. The tumors radii taken are 2.5 cm, 3.5 cm and 4.5 cm. Figure 48 depicts the simulated return loss results. It can be noticed that the values of the return loss of these different cases fluctuate around that of the normal breast, but they differ from one another depending on the size of the tumor. These patterns indicate that there is a cancerous tumor inside the breast which falls within stage II.

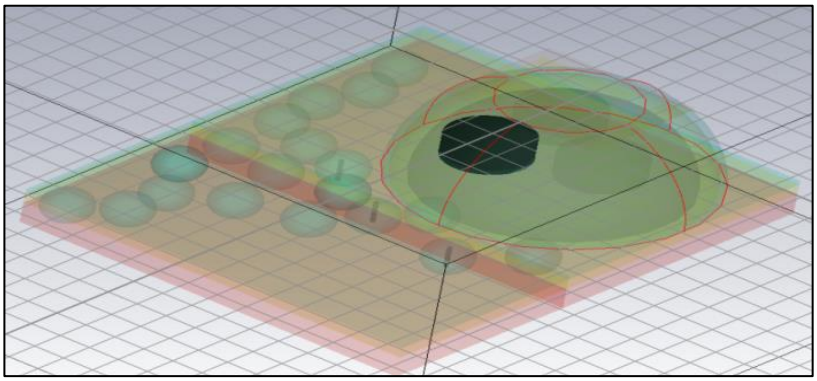

Figure 47: Three tumors in breast Case 3

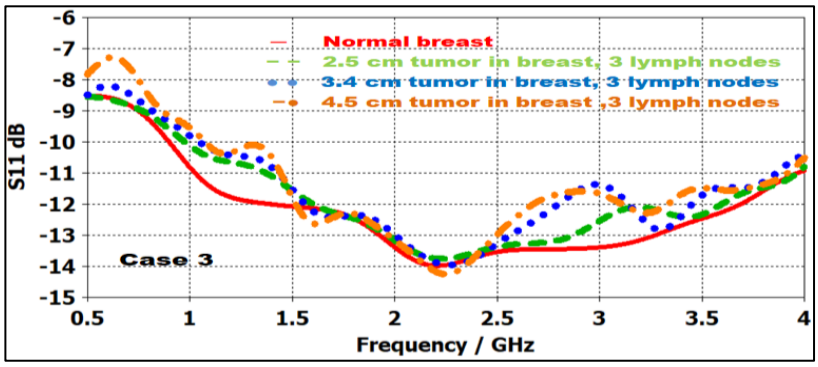

Figure 48: Simulated return loss for Case 3

In Case 4, there are five tumors within the breast in addition to three tumors in the lymph nodes. The tumors radii taken were 2.5 cm, 3.5 cm and 4.5 cm; similar to Case 3.

In case 5, there are eight tumors within the breast. The tumors are illustrated in Figure 49 and Figure 50 for Case 4 and Case 5 respectively. For Case 5, only the results for radii 2.5 cm and 3.5 cm are presented. The return loss are depicted in Figure 51 and Figure 52 respectively.

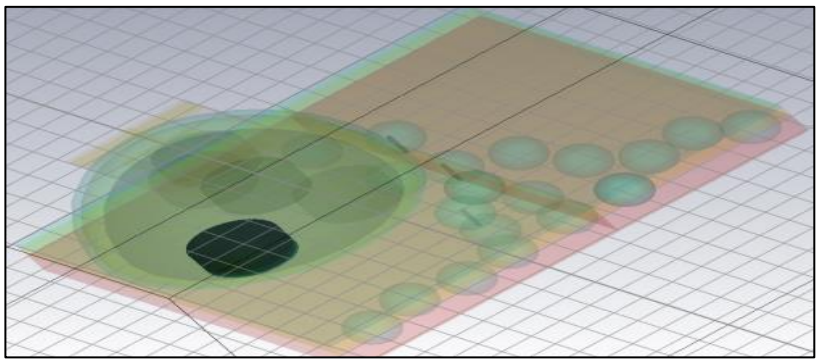

Figure 49: Five tumors in breast, Case 4

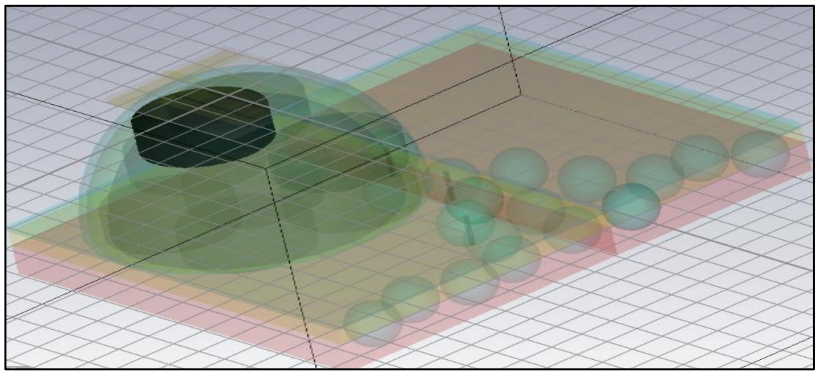

Figure 50: Eight tumors in breast, Case 5

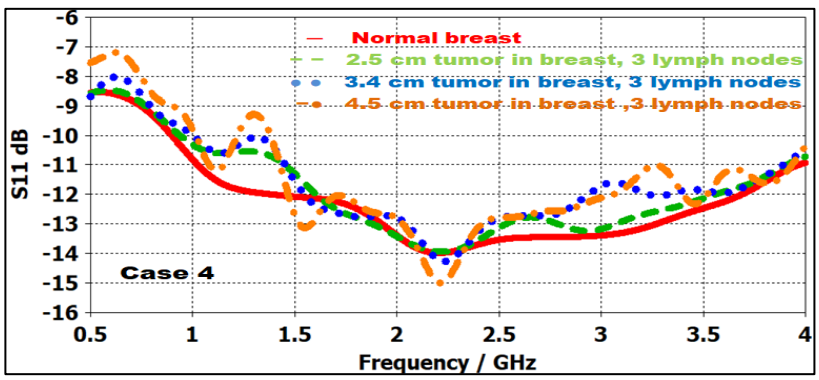

Figure 51: Simulated return loss for Case 4

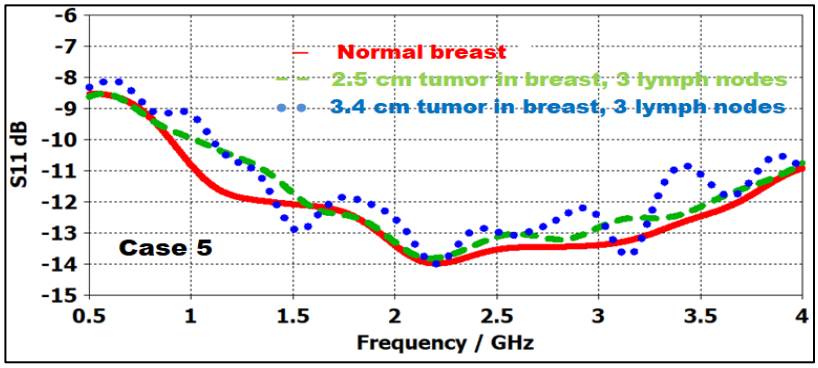

Figure 52: Simulated return loss for Case 5

In Case 6, tumors are considered to be within the breast only, with radius greater than 5 cm as show in Figure 53. The tumors radii taken were 6 cm, 7 cm and 8 cm. Figure 54 depicts the simulated return loss results for Case 6.

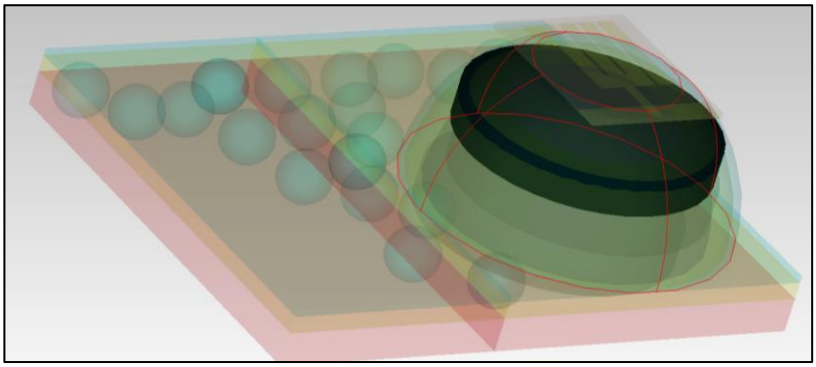

Figure 53: Tumors in breast, Case 6

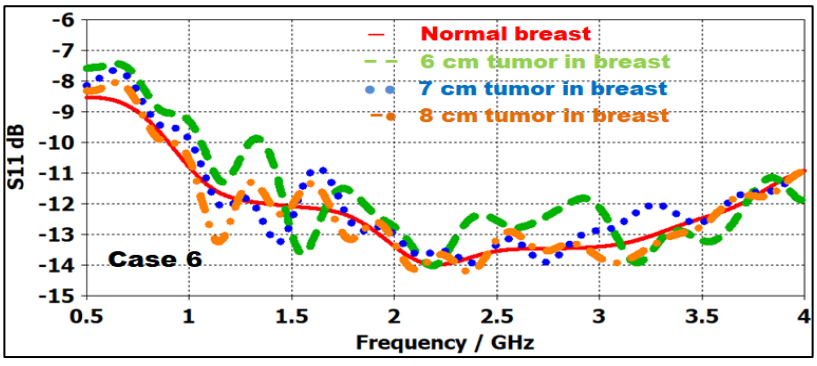

Figure 54: Simulated return loss for Case 6

In addition to the discrepancy in return loss values in the cases study for stage II breast cancer, it is worth noticing that other antenna parameters also reveal differences. Table8 depicts the average directivity (D_o) and gain (G_o) for these different cases at 2.25 GHz.

The results show that Cases 1, 2, and 3 have similar properties. Cases 4 and 5 differ from the previous cases but resemble one another. Case 6 has distinct characteristics.

Table 8: Average directivity and gain

Cancer case	G_o	D_o
Case 1	-14.29	5.898
Case 2	-14.68	5.522
Case 3	-14.76	5.273
Case 4	-15.68	4.59
Case 5	-15.38	4.708
Case 6	-12.36	6.821

It is important to point out that the computational time for most of the simulations is within range from 15 to 38 minutes depending on the substrate details of layers and tumors in breast. The available personal computer has RAM of 8 GB.

5.4 Specific Absorption Rate (SAR)

Since the antenna is designed to be used on a human body, the Specific Absorption Rate (SAR) of the human tissues should be taken into consideration. SAR is a measure of the absorption of electromagnetic energy in the body, in watts per

kilogram (W/kg). Hence, the lower the SAR achieved, the better. The main factors that affect the absorption rate are the power transmitted and the antenna position. SAR is a function of sample conductivity (σ), mass density of the tissue (m_d) and the RMS of electric field component (E) [50].

$$SAR = \frac{\sigma^* \mathrm{E}^2}{m_d} \tag{5.1}$$

SAR generally has two standardized limits.

- The US peak limit for general public is 1.6 W/kg over 1 g of tissue with an exposure time of 30 minutes.
- The European peak limit is 2 W/kg over 10 g of tissue within 6 minutes of exposure time [34].

For the average worker, the safety zone is less than 0.4 W/kg with controlled exposure (6 minutes at a time).

In this study the value of SAR is calculated by using CST. Mass density of the skin, fat and glandular tissues in the models have been taken as 972 kg/m^3, 890 kg/m^3 and 900 kg/m^3 respectively [35] and the average SAR are determined and depicted in Figures 55 & 56 for the planar [3] and spherical breast models [4].

The SAR values detected are 0.155 and 0.145 W/kg which are significantly lower than the safety parameters [34, 35].

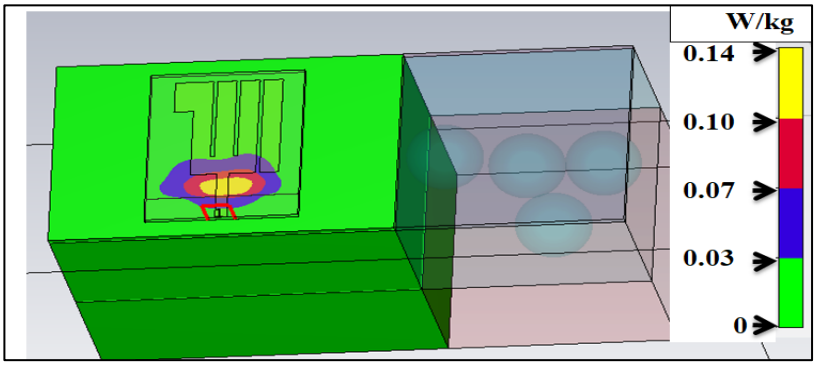

Figure 55: Simulated SAR for the antenna implanted on the planar breast model [3]

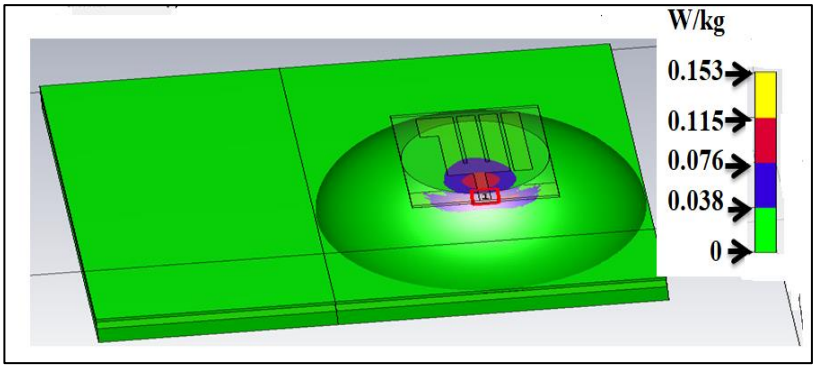

Figure 56: Simulated SAR for the antenna implanted on hemispherical breast model [4]

5.5 Validation of the Results and Discussion

In this study, we focused on deviations in the return loss as a method for detection of cancerous cells in six different cases. It is worth mentioning that the antenna directivity and gain are used to support the preliminary indication of existence of cancer cells as summarized in Table 8. In this approach, a simple measurement setup is considered by using a vector network analyzer. The method is verified by comparing the measured return loss of the designed antenna implanted on a normal female breast; where average values are adopted, with different breast model simulation results.

These results include a planar breast model composed of parallel breast layers [3] and a hemispherical model resembling the real breast shape associated with neighboring parts and lymph nodes [4]. The simulation results show that both models are in good agreement with the measured results of a female human breast. However, hemispherical shaped model's results are closer, validating that the modeled breast has similar properties of the female human breast. Then, the effect of the electrical parameters of the malignant tissues were studied for different stage II cases when adding different number of the malignant tissues with different distribution in either the breast or the lymph nodes or both at the same time.

In the adopted technique the measurement can be done directly on the body avoiding distraction from the mechanical supports or any other object around the setup. In the same time, there is no need for adding absorbing material over all surroundings. Furthermore, it is independent from how weak the scattered field is or is a transformation of the scattered field required to verify the measured results. Moreover, if all medical and health restrictions are taken into consideration there is no need for a phantom to be used. Instead, the measurement can be carried out directly on the infected body. The average values of SAR are calculated to ensure safe operations.

Concerning similar methods of cancer diagnosis, Akyuz and et. al developed a model based on the scattered field from a human breast phantom using two rotating antennas for transmission and reception [36]. One of the main points on this approach, is that the multi-frequency measurement is very adequate to cover the frequency dependence of the complex dialectic permittivity of biological tissues. Similarly, Shokry and Allam studied UWB antenna for brain stroke and brain tumor

detection based on the simulated return loss of the brain model and the measurements on the brain phantom [38]. UWB antenna has also been used for the detection of lung cancer [30].

Other published articles based on the same concept of return loss imaging for cancer detection used different antennas on different body organs like breast, brain, oral and lung [26-30], [37-38] are available in the literature. The frequency shift of the return loss of the infected organ is a common observation in all cases.

On the other hand, we should point out that some publications are tackling the same issue using time-domain-based imaging which is cost effective and fast. However, they are subject to errors due to fast sampling rate. On the contrary, the adopted antenna is simple to fabricate and the results are verified on the human body. The return loss for the infected organ can be measured if all medical safety constraints are achieved [39–40].

5.6 Conclusion

In this chapter, the designed antenna is place on female human breast with hemispherical shape model having closer characteristics to the real human breast. The return loss is measured and simulated in free space and on a real human breast. The antenna is used to detect the effect of malignant tissues in the breast on the antenna via measuring the antenna performance namely; return loss, directivity and gain. It is worth noticing that depending on the number of tumors and their spread; either within the lymph nodes or the breast, each case of stage II breast cancer can be detected and accurately assessed. It is important to note that the return loss of the antenna on a real breast is identical to that of the simulated model using CST.

The Specific Absorption Rates detected during the simulation are within acceptable limits. The recorded SAR values where 0.14 W/kg and 0.15 W/kg for the antenna implemented on the planar breast model and the hemispherical breast model receptively. These values are considered safe according to the IEEE SAR standard values depending on number of cancer tissues, its size and its location either on breast or in lymph-nodes and the arm. The proposed approach gives a discrepancy both in the antenna return loss and directivity as described in six different case studies.

It is important to point out that the antenna chosen has a simple structure and is a good sensor to exhibit the effect of cancer tissues on the return loss, directivity and gain. This sensing approach is not based on time-domain-based imaging which is cost effective but subject to error due to fast sampling rate.

Chapter 6

CONCLUSION

The thesis outlines the breast cancer detection using the electromagnetic properties of multiple layers of the human breast. The dielectric constant, conductivity and thickness of each layer are specified for the normal breast tissues of these organs and also for the infected ones. Most of these properties are found in biological and bioengineering articles. There is a significant variance of these electrical properties from layer to another layer and from normal to infected body which will alter the scattering properties of the electromagnetic wave impinging on this part of the human body. The study is presented in Industrial, Scientific, and Medical (ISM) frequency band (2.4 GHz to 2.4835 GHz).

An antenna having different bricks of copper annealed implemented on FR4 substrate with relative dielectric constant 4.3, thickness 1.6 mm, cross sectional area 5×4 cm^2 and loss tangent 0.025 is designed and fabricated. The antenna is excited using microstrip line of 50 Ω for good matching with the source. The return loss variations due to breast material and vacuum are compared.

The antenna sensor is placed on the breast and different return loss responses are obtained for the normal and malignant tissues.

Two human breast models are introduced in this work, a model in a form of multilayer planar structure consists of three layers, skin, fat and glandular with

relative dielectric constants and electrical conductivities of 38, 1.46, 5.15, 0.138, 57.2 and 1.9 respectively. The lymph layers are skin, fat and muscles with relative dielectric constant and electrical conductivity of 38.006, 1.464, 5.28, 0.105, 53.75 and 1.81. The relative dielectric constant and electrical conductivity of the lymph node itself is 78 and 0.965 respectively. The second one is a novel model in a form of hemispherical multilayer structure, having closer characteristics to a real human breast. For the both models the return loss is measured and simulated in free space and on the real human breast. The antenna is used then to detect the effects of malignant tissues in the breast via measuring the antenna performance namely; return loss, directivity and gain.

For antenna implanted on planar breast model without lymph nodes (stage 1A) different structures and number of turns are studied. The tumor radius values of 0.5 cm, 1.0 cm, 1.5 cm and 2.0 cm are considered. For each value of tumor radius, the tumor depth takes the values 1.0 cm, 2.0 cm and 3.0 cm. On the other hand, number of tumors in each layer is changed to be 1, 3, and 5. For antenna implanted on planar breast model with lymph nodes (stage 1B) the same structures and number of tumors in breast but are studied, adding tumor cells in lymph nodes of radius 1.9mm. It is concluded that increasing the tumor radius either shifts the resonance or change the values of the return loss. Moreover, increasing the number of tumors cells increases the discrepancy of the return loss image. On the hand the adopted analysis can sense the case of very early stage of the initial case of cancer in the body. For the hemispherical shaped breast model, tumors in breast and lymph nodes with different sizes and numbers are used to illustrate the second stage of cancer diagnosis.

The return loss measurements are taken by using a network analyzer. Separate measurements are taken in free space and when placed on a healthy human breast. Simulations carried out by CST Microwave Studio and normal breast models are in a good agreement with the measured results. The presented work is shown to be very accurate for breast cancer detection thereby reducing the need for invasive surgical operations.

It is concluded form the analysis of the planar model that increasing the tumor radius either shifts the resonance or change the values of the return loss. Moreover, increasing the number of tumors cells increases the discrepancy of the return loss image. On the hand the adopted analysis can sense the case of very early stage of the cancer in the body. Concerning the second model analysis one can conclude that depending on the number of tumors and their spread within the lymph nodes or the breast, each case of stage II cancer can be detected and accurately assessed. It is important to note that the return loss of the antenna on a real breast is identical to that of the simulated model using CST. The Specific Absorption Rates detected during the simulation were within acceptable limits.

Chapter 7

FUTURE WORK

The effects of different types of antennas will be examined considering the dispersive behavior of the breast and tumors. Implementing phantoms for infected bodies may also be studied for confirming the measured results of infected body. Also, real measurements are needed on real infected people have to be carried out. Several antennas with high accuracy should be used for cancer detection . Among them, Flexible antenna, Circular Patch Antenna, and Ultra Wideband (UWB) Antenna.

REFERENCES

[1] Rahmat-Samii, Y., & Kim, J. (1955). Implanted Antennas in Medical Wireless Communications. *A Publication in the Morgan and Claypool Publishers' series, 1st edition. Trans. Roy. Soc. London*, vol. A247, 1995, pp. 529–551 April 1955.

[2] American Cancer Society. (2013). Cancer facts and figures. Retrieved from http://www.cancer.org/acs/groups/content/@epidemiologysurveilance/documents/document/acspc-036845.pdf

[3] Ali, N., Uyguroglu, R., & Allam, A.M.M.A. (2018). Cancer diagnosis in breast using biological and electromagnetic properties of breast tissues on antenna performance.The *IEEE 18th Mediterranean Microwave Symposium; MMS* 2018, *Istanbul, Turkey*, November. 2018.

[4] Ali, N., Uyguroglu, R., Abo Sree, M.F., & Allam, A.M.M.A. (2020). Stage II cancer diagnosis using printed antenna implanted on hemispherical model for human breast. *Journal of Instrumentation, Published 14 September 2020 • © 2020 IOP Publishing Ltd and Sissa Medialab.*

[5] Lin, J.C., & Wang, Y.J. (1987). An implantable microwave antenna for intertribal hyperthermia. *Proceedings of IEEE*, vol. 75, no. 8, pp. 1132-113, Aug. 1987.

[6] Rao, S.M.N., Mharte, A., Popa, D.O., Chiao, J.C., Ativanichayaphong, Sin, T.J., & Stephanou, H.E. (2005). *MEMS based implantable drug delivery system. VII*

International Conference on Micro Electro Mechanical Systems, El Paso, TX, USA and Ciudad Juarez, Mexico, pp. 1-4. Sep. 21-22, 2005.

[7] Merli, F. (2011). Implantable antennas for biomedical applications. Ph.D. dissertation, Dept. Elect. Eng., EPFL Univ., Lausanne, Switzerland.

[8] Sagan, D. (2007). RF integrated circuits for medical applications: Meeting the challenge of ultra-low power communication. Retrieved from. http://stf.ucsd.edu/presentations/2007/2007-08%20STF%20-%20Zarlink%20ULP%20transceivers.pdf.

[9] Durney, C.H & Iskander, M. F. (1988). Antennas for medical applications, in Antenna Handbook, Y.T. Lo and S.W. Lee, Eds. New York: Van Nostrand, Ch. 24.

[10] Rosen, A., Stuchly, M. A., & Vorst, A.V. (2002). Applications of RF/microwaves in medicine. *IEEE Trans. Microwave Theory Tech.,* vol. 50, no. 3, pp. 963–974, Mar. 2002.

[11] Steinhaus, B.M., Smith, R.E., & Crosby, p. (1994). The role of telecommunications in Future implantable device systems. *16th IEEE EMBS Conf., Baltimore,* MD, pp. 1013–1014, 1994.

[12] Anders J Johansson. (2004). Wireless Communication with Medical Implants: Antennas and Propagation. pp.19-20, 2004.

[13] Zhi Ning Chen, G.C.L, & See, T.S.P. (2009). Transmission of rf signals between Mics loop antennas in free space and implanted in the human head. *IEEE Transactions on Antennas and Propagation*, vol. 57, No. 6, p. 4, 2009.

[14] Loren Schwiebert, J.W., Sandeep., & Gupta, K.S. (2009). Research challenges in wireless networks of biomedical sensors, *In Proceedings of the 7th annual international conference on Mobile computing and networking (MobiCom '01*). ACM, New York, NY, USA, p. 15, 2001, Antennas and Propagation, vol. Vol. 57, No. 6, p. 4, 2009.

[15] Soykan, D. O. (2002). Power sources for implantable medical devices, tech. rep. Michigan Technological University, 2002.

[16] Hackworth, S. A. (2010). Design, optimization and implementation of a volume conduction energy transfer platform for implantable devises. PhD thesis, University of Pittsburgh, 2010.

[17] Valero, J. G. (2011). Multiband and Silicon Integrated Antennas for Wireless Sensor Networks. PhD thesis, Universidad Autonoma de Barcelona, 2011.

[18] Couty, M., Woytasik, M., Ginefri, J.-C., Rubin, A., Martincic, E., Darrasse, M., Boumezbeur, L.F., Lethimonnier, F., Tatouli, M., & Dufour-Gergam, E. (2012). Fabrication and packaging of flexible polymeric micro antennae for in vivo magnetic resonance imaging. *Polymers.* vol. 4, pp. 656–673, 2012.

[19] El-bahii, M.M. (2015).Diagnosis of lung cancer using electric properties of lung tissues. Bachelor Thesis. German University in Cairo, 2015.

[20] Dijana, L. P., Leah, M. B., Cynthia, W., Mary, J. L., Josephine, H., Sarah, S., Travis, O., Anthony, M., Tara, M.B., Walley, T., Daphne, M., John, H.B., Michal, O., & Susan, C.H. (2007). A large-scale study of the ultra-wide band microwave dielectric properties of normal, benign and malignant breast tissues obtained from cancer surgeries, *Phys. Med. Biol.*, vol.52, pp. 6093–6115, Oct. 2007.

[21] Balanis, C.A. (1997). Antenna Theory. Analysis and Design. 2nd ed. John Wiley & Sons. 1997.

[22] Abdelsayed, S.M., Nikolova, N.K., & Deen, M.J. (2005).Radiation Characteristics of Loop Antennas for Biomedical Implants. Proceedings of the XXVII General Assembly of the International Union of Radio Science (URSI) General Assembly, New Delhi, India. 4 pages (23 - 29 October 2005).

[23] Khaleghi, A., & Balasingham, I. (2009). On the Ultra Wideband Propagation Channel Characterizations of the Biomedical Implants. *IEEE, VTC Spring* 2009, pp. 1-4, doi: 10.1109/VETECS.2009.5073740. 2009.

[24] Kim, J., & Rahmat-Samii,Y. (2004). Implanted Antennas inside a Human Body: Simulations, Designs, and Characterizations. *IEEE Transactions on Microwave Theory and Techniques*, vol.52, no.8, pp.1934-1943, August 2004.

[25] IEEE Standard for Safety Levels with Respect to human Exposure to Radio Frequency Electromagnetic Fields, 3kHz to 300 GHz, IEEE Standard C95.1-1999,1999

[26] Hanafy, E.A., & Allam, A.M.M.A. (2004). Investigation for Breast Cancer Using Antennas in the ISM Frequency Band*", IEEE Conference on Antenna Measurements & Applications (CAMA), France,* November, 2014.

[27] Abbassi, P. K., Allam, A. M. M. A., & Abdelkader, R. M. (2014). Design and Implementation of Implanted antenna Inside a Human Body. *IEEE Conference on Antenna Measurements & Applications (CAMA), France,* November, 2014

[28] Gabriel, C. S. (1996). Compilation of the dielectric Improving in-body ultra-wide-band communication 13 properties of body tissues at RF and microwave frequencies. Brooks Air force Tech. Rep AL/OE-TR-1996-0037, 1996.

[29] Robert Ferrer, M. D., M. P. H. (1998). Lymphadenopathy Differential Diagnosis and Evaluation. Texas. Am Fam Physician, 1998.

[30] Porter, E., Fakhoury, J., Oprisor, R., Coate, M., & Popovićs, M. (2010). Improved Tissue Phantoms for Experimental Validation of Microwave Breast Cancer Detection", *European Conference on Antennas and Propagation*, 2010.

[31] Houzen1, T., Takahashi2, M., & Ito, K. (2007). Implanted Antenna for an Artificial Cardiac Pacemaker System. Progress in Electromagnetics Research Symposium. Prague, Czech Republic, August 27-30, 2007.

[32] Johansson, A. J. (2004) .Wireless Communication with Medical Implants: Antennas and Propagation, June 2004.

[33] Khaleghi, A., & Balasingham, I. (2009). On the Ultra Wideband Propagation Channel Characterizations of the Biomedical Implants. *VTC Spring 2009 - IEEE 69th, pp. 1-4, doi: 10.1109/VETECS*.2009.5073740.

[34] Seabury, D. (2005). An update on SAR standards and the basic requirements for SAR assessment. *ETS-Indgren,* p. 8, 2005.

[35] Hopp, T., Ruiter, N., Bamber, J. C., Duric N., & Dongen, K. W. A. (2017). Procceding of Inernational Workshop on Medical Ultrasound Tomography. *Speyer Germany*, Nov. 2017.

[36] Gurbuz, T. U., Aslayurek, B., Yapar, A., Sahinturk, H., & Akduman, İ. (2014). A nonlinear Microwave Cancer Imaging Approach through Realistic Body-Breast Modelling. *IEEE Trans. On Antenna and Propag,*Vol. 62, No. 5, May 2014.

[37] Allam, A. M. M. A., & Badawy, M. M. A. (2016). Detection of Lung Cancer Using Ultra Wide Band Antenna. *Loughborough Antennas Propagation Conference (LAPC), (IEEE),* UK14-15, Nov. 2016.

[38] Shokry, M. A., & Allam, A. M. M. A. (2016) UWB Antenna for Brain stroke and Brain Tumor Detection. *MRW2016 MIKON2016/IRS2016), Poland,* 9-11 May 2016.

[39] Sugitani, T., Kubota, S., Toya, A,. Xiao, & X., Kikkawa, T. (2013).A compact 4times4 planar uwb antenna array for 3-d breast cancer detection. *IEEE Antennas and Wireless Propagation Letters,* vol. 12, pp. 733–736, 2013.

[40] Islam, M. T. Samsuzzaman, M., Kibria, S., Misran, N., & Islam, M. T. (2019). Metasurface loaded high gain antenna based microwave imaging using iteratively corrected delay multiply and sum algorithm. Scientific reports, vol. 9, no. 1, pp. 1–14, 2019.

[41] Kwon, S., & Lee, S. (2013). Instantaneous microwave imaging with time-domain measurements for breast cancer detection. Electronics Letters, vol. 49, no. 10, pp. 639–641, 2013.

[42] Porter, E. Bahrami, H., Santorelli, A., Gosselin, B., Rus L. A., & Popovi ć, M. (2016).wearable microwave antenna array for time-domain breast tumor screening. *IEEE transactions on medical imaging,* vol. 35, no. 6, pp. 1501–1509, 2016.

[43] Islam, M.T. Samsuzzaman, M., Islam, M., Kibria, S., & Singh et al., M. J. (2018). A homogeneous breast phantom measurement system with an improved modified microwave imaging antenna sensor. Sensors, vol. 18, no. 9, p. 2962, 2018.

[44] Rahman, A. M., Islam, T., Singh, M. J., Kibria, S., & Akhtaruzzaman, M. (2016) .Electromagnetic performances analysis of an ultra-wideband and flexible

material antenna in microwave breast imaging: to implement a wearable medical bra", Scientific reports, vol. 6, p. 38906, 2016.

[45] Song, H., Sasada, S., Kadoya, T., Okada, M., Arihiro, K., Xiao, X., & Kikkawa, T. (2017). Detectability of breast tumor by a hand-held impulse-radar detector: performance evaluation and pilot clinical study.scientific reports, vol. 7, no. 1, pp. 1–11, 2017.

[46] Salvador, S. M., Fear, E. C., Okoniewski, M. J., & Matyas, R. (2010). Exploring joint tissues with microwave imaging. *IEEE Transactions on Microwave Theory and Techniques* , vol. 58, no. 8, pp. 2307–2313, 2010.

[47] Porter, E., Kirshin, E., Santorelli, A., Coates, M., & Popovi ć, M. (2013). Time-domain multistatic radar system for microwave breast screening. *IEEE Antennas and Wireless Propagation Letters,*vol. 12, pp. 229–232, 2013.

[48] Kibria, S., Samsuzzaman, M., Islam, M. T., Mahmud, M. Z., Misran, N., & Islam, M. T. (2019). Breast phantom imaging using iteratively corrected coherence factor delay and sum. *IEEE Access*, vol.7, pp. 40822–40832, 2019.

[49] Mahmud, M. Z., Islam, M. T., Misran, N., Kibria, S., Sam, M., & suzzaman. (2018). Microwave imaging for breast tumor detection using uniplanar amc based cpw-fed microstrip antenna. *IEEE Access*, vol. 6, pp. 44763–44 775, 2018.

[50] Kumari,V., Sheoran, G., & Kanumuri T. (2019). SAR analysis of directive antenna on anatomically real breast phantoms for microwave holography. Microwave and optical Technology Letters 62, 466-473, 13 September 2019.

APPENDIX

Antenna Design

A. This appendix is devoted of design step of antenna adaptivo in this theise as follows:

1. Implementing the traditional patch antenna shown in figure A1 of width W and length L using equations (a-1) and (a-2)[21]

The width

$$W = \frac{c}{2f_{\circ}\sqrt{\frac{(\varepsilon_r + 1)}{2}}} \qquad [\text{A-1}]$$

The actual length (L)

$$L = L_{eff} - 2\Delta\text{L} \qquad [\text{A-2}]$$

where

$$\varepsilon_{reff} = \frac{\varepsilon_r + 1}{2} + \frac{\varepsilon_r - 1}{2}(1 + 12\ h/W)^{-1/2}$$

the effective length (L_{eff})

$$L_{eff} = \frac{c}{2f_{\circ}\sqrt{\varepsilon_{reff}}}$$

Fringing length (ΔL)

$$\Delta\text{L} = 0.412h\frac{(\varepsilon_{reff} + 0.3)(\frac{W}{h} + 0.264)}{(\varepsilon_{reff} - 0.258)(\frac{W}{h} + 0.8)}$$

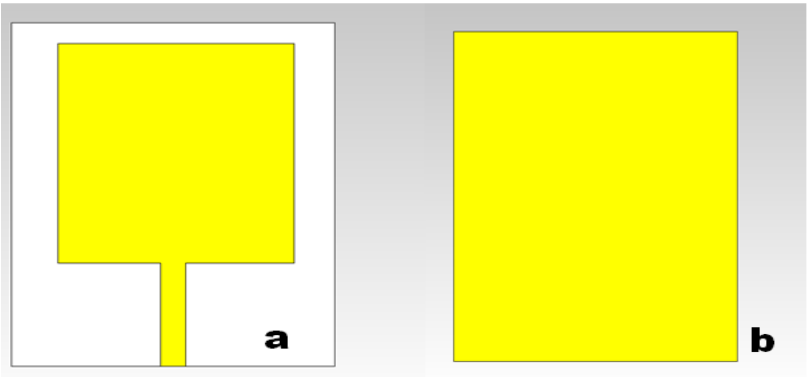

Figure A.1: Traditional patch antenna. (a) top view (b) bottom view

2. Modify the antenna by subtracting different strip with different length and width as shown in Figure A2.concsrning this step the return loss for different configuration of antenna in free space are depicted in Figure A3.

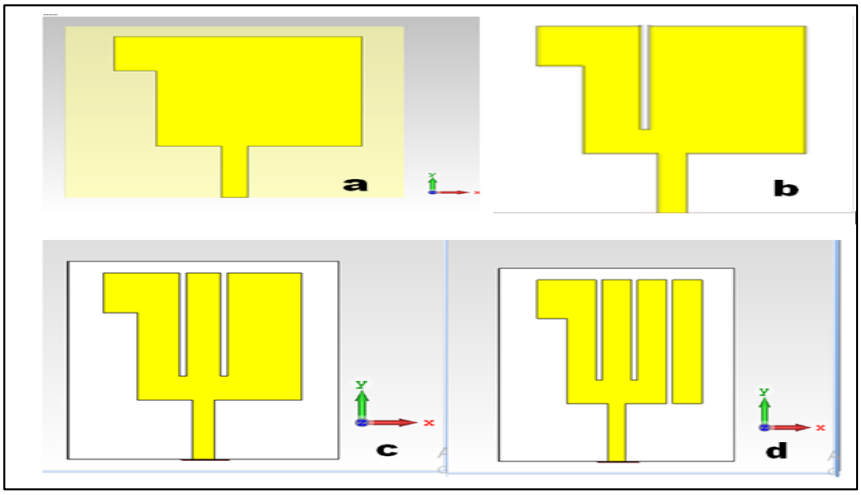

Figure A.2: Modification of convention patch

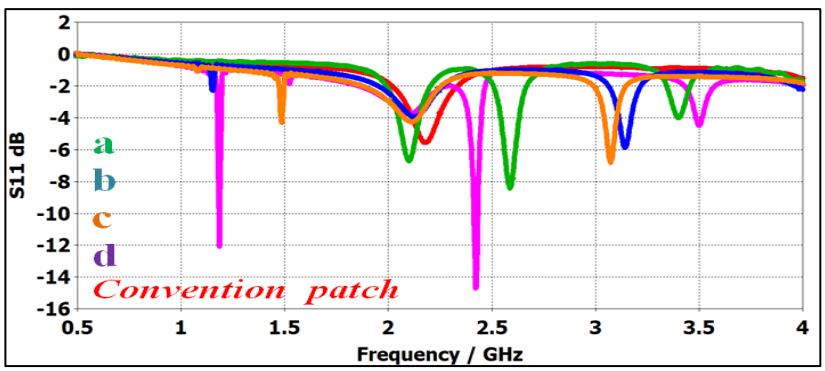

Figure A.3: The return loss for different configuration of microsrip patch antenna in figure A2

3. Change the ground length from lg =8mm up to lg =42 and put the antenna on normal breast to achieve resonate frequency around 2 .11 Ghz. It is clear that lg=8mm is the best one.

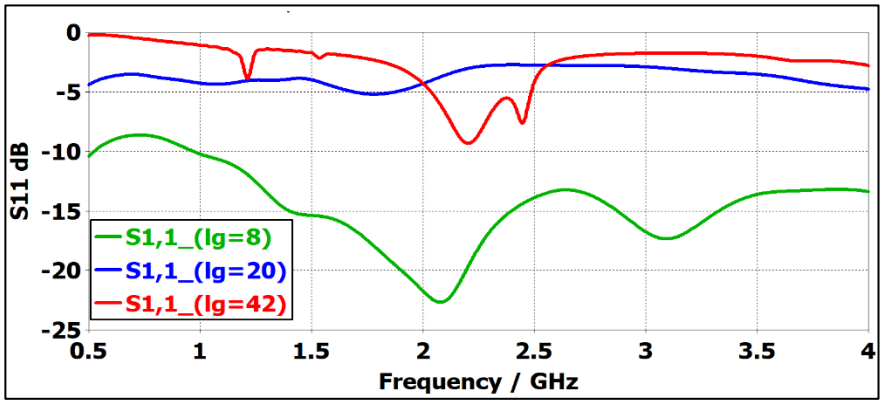

Figure A.4: The return loss for modify antenna on normal breast